REDETERMINATION OF THE STRUCTURE OF K_2SnBr_6 AT ROOM TEMPERATURE

by

S. NARASINGA RAO, M.Sc.

A Thesis

Submitted to the Faculty of Graduate Studies

in Partial Fulfilment of the Requirements

for the Degree

Master of Science

McMaster University
August 1969

MASTER OF SCIENCE (1969)
(Physics)

McMASTER UNIVERSITY
Hamilton, Ontario

TITLE: Redetermination of the Structure of K_2SnBr_6 at room temperature.

AUTHOR: S. Narasinga Rao, B.Sc. (Madras)

M.Sc. (Madras)

SUPERVISOR: Dr. I. D. Brown

NUMBER OF PAGES: vi, 68

SCOPE AND CONTENTS:

The crystal structure of K_2SnBr_6 has been reinvestigated using single crystal x-ray diffraction techniques. Three dimensional intensity data obtained photographically have been used to refine the structure, by the least square analysis. The structure is found to be slightly distorted from the regular cubic K_2PtCl_6 structure in a manner similar to K_2TeBr_6. The Sn-Br bond is found to be 2.601 Å.

The structure of K_2SnBr_6 is found to be monoclinic with space group $P2_1/n$ and $a = 7.435 \pm 0.017$ Å, $b = 7.437 \pm 0.017$ Å, and $c = 10.568 \pm 0.006$ Å.

A review of other crystals with similar structure is included in this thesis and the theory of x-ray diffraction and crystal structure as applicable to the present problem is discussed briefly.

REDETERMINATION OF THE STRUCTURE OF K_2SnBr_6 AT ROOM TEMPERATURE

by

S. NARASINGA RAO M.Sc.

REDETERMINATION OF THE STRUCTURE OF K_2SnBr_6 AT ROOM TEMPERATURE

ACKNOWLEDGEMENTS

I should like to express my sincere appreciation and gratitude to Dr. I. D. Brown for his encouragement and guidance throughout the course of this work.

Thanks are due to Dr. C. Calvo and to all my friends and colleagues in the group for suggestions, assistance and helpful discussions at various stages of this work.

Thanks are also due to the National Research Council of Canada for supporting this work and to the McMaster University for a graduate scholarship.

My thanks are due to the Madras Christian College Council for granting me study leave for this period.

Table of Contents

LIST OF DIAGRAMS

FIGURE

LIST OF TABLES

Chapter 1

INTRODUCTION

The structures of a large number of crystals having the general formula R_2MX_6 where R is an alkali metal, M is a four valent metal and X is a halogen have been solved using x-ray diffraction techniques, mostly the powder method.[1-6] Most of these crystals are found to crystallise in the cubic potassium hexachloroplatinate (K_2PtCl_6) structure[1], space group $Fm\bar{3}m$ (O_h^5). The K_2PtCl_6 structure is basically an antifluorite structure in which the regular octahedral anions ($PtCl_6^{2-}$) are arranged on a face centered cubic lattice while each cation (K^+) occupies the tetrahedral interstices formed by neighbouring ions (See Fig. 1). The platinumchlorine bonds lie along the principal axes of the cubic unit cell. Each K^+ ion in this structure is surrounded by twelve chlorine atoms at the same distance from it.

However, a few of these structures have been found to distort slightly from the regular K_2PtCl_6 structure. Brown[7] has reported such a distortion in K_2TeBr_6 while Brown and Lim[8] have observed a similar distortion in K_2PbCl_6.

Ketallar, Rietdijk and van Staveren[9] and Markstein

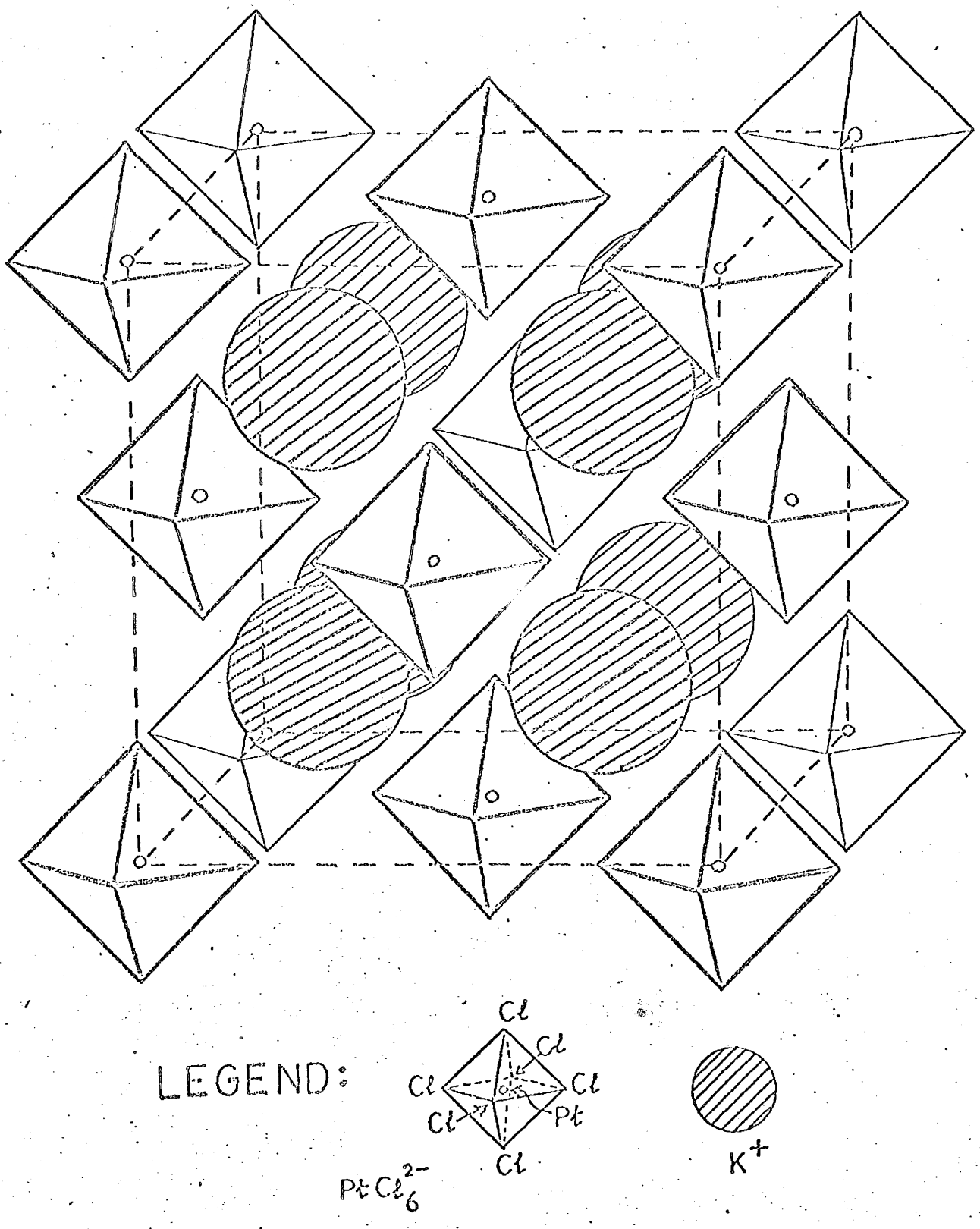

Fig. 1. The unit cell of Potassium hexachloroplatinate, K_2PtCl_6

and Nowotny[10], using single crystals, have studied the symmetry of K_2SnBr_6. According to Ketallar et al, K_2SnBr_6 is cubic and has the K_2PtCl_6 structure with $\underline{a} = \underline{b} = \underline{c} = 10.48$Å. According to Markstein and Nowotny, it is tetragonal, pseudo-cubic, Space group $C42_12$ with a slightly distorted K_2PtCl_6 structure and with $\underline{a} = \underline{b} = 10.51$ Å. The primitive tetragonal cell has space group $P42_12$ with the dimensions $\underline{a} = 7.43$ Å and $\underline{c} = 10.61$ Å. Galloni, De Benyacar and De Abeledo[11], using powder photographs, have found that the cell, tetragonal at room temperature becomes cubic at 126.5°C with $\underline{a} = 10.61$ Å at 130°.

The study of Nuclear Quadrupole Resonances and the thermal behaviour of some of these complexes has also led to the observation that similar distortions do exist in many of them. Nakamura et al[12-16] have used the quadrupole resonance of halogens to examine the hexahalogenate anions of a number of metals such as Pt(IV), Sn(IV), Te(IV) and Re(IV). In many cases, they have reported the splitting of the resonance signals which indicates the presence of nonequivalent halogen atoms in these structures. Such structures must, therefore, have symmetries lower than cubic. In particular, they[17] observed the pure quadrupole resonance of bromine in potassium hexa bromostannate. The bromine nuclear quadrupole resonance line is split into a triplet, indicating the presence of at least three kinds of non-equivalent bromine atoms in the crystal suggesting that the true symmetry is

lower than tetragonal.

Morfee, Staveley, Walters and Wigley[18] have carried out the measurements of heat capacities of complexes $(NH_4)_2SnCl_6$ and $(NH_4)_2SnBr_6$, at low temperatures. Both these are found to have the K_2PtCl_6 structure at room temperature, but exhibit specific heat anomalies between 100°K and 300°K. The authors have suggested that some distortions might occur in these compounds. The anomaly in $(NH_4)_2SnCl_6$ is small and occurs between 235°K and 245°K and it is unlikely that a change in structure is involved. But the contrary is the case for $(NH_4)_2SnBr_6$, where the anomaly is large. Busey, Dearman and Bevan Jr.[19] have noticed the anomalies in specific heat in K_2ReCl_6 at 76°C, 103°C and 111°C and they suggest that these are due to some distortions in the structure of this compound. Furthermore, the neutron diffraction study of K_2ReCl_6 by Smith and Bacon[20] has confirmed the change in the symmetry from the space group Fm3m at room temperature to a space group of lower symmetry Pn3 or Pn3m, even though it still remains cubic below 77°C. Busey and his co-workers[21] have also reported the specific heat anomalies in K_2ReBr_6 at 225°K and 245°K. Templeton and Dauben[6] have found this compound to have the K_2PtCl_6 structure at room temperature. Ikeda, Nakamura and Kubo[22-23] have found from nuclear quadrupole resonance that it undergoes three close transitions below 270°K.

Brown[7] has proposed an explanation for such distor-

tions. He suggests that if the cation is very much smaller than the cavity into which it fits, the anions will re-orient themselves in such a way as to reduce the effective cavity size and thus lock the cation in place. Morfree, Staveley, Walters and Wigley[18] have also made a similar suggestion to account for the specific heat anomaly in $(NH_4)_2SnBr_6$ at low temperature. Brown has further given a criterion to decide whether any given structure is expected to be distorted from the regular K_2PtCl_6 structure or not. This criterion is based on the "radius ratio" which is defined as the ratio of the cation radius to the radius of the cavity formed by twelve halogen atoms surrounding it. He has observed that,

i. Crystals with a radius ratio of less than about 0.89 are distorted from the cubic structure at room temperature;

ii. Crystals with a radius ratio between 0.89 and 0.98 are cubic at room temperature but distort at lower temperature;

iii. Crystals with a radius ratio greater than 0.98 are not distorted from the cubic structure at any temperature.

The structures of some crystals of the type R_2MX_6, arranged in the order of radius ratio are listed in Table A.

This thesis describes the refinement of the crystal

TABLE A

Structures of Some R_2MX_6 type crystals

Compound	Radius Ratio	Structure	Method: X-RAY	Method: NQR	Method: Specific heat
1. Crystals which are distorted from cubic at room temperature					
K_2TeBr_6	0.83	Monoclinic at 293°K	7	13	
K_2SnBr_6	0.86	Tetragonal at 293°K, Cubic above 400°K, Monoclinic at 293°K	10,25 24	14	18
Rb_2TeI_6	0.86	Tetragonal at 293°K, Cubic above 328°K.		16	
K_2TeCl_6	0.89	Monoclinic at 293°K	2	13	
K_2PbCl_6	0.91	Monoclinic at 300°K, Cubic above 333°K.	8		
2. Crystals which are cubic at room temperature but distorted at low temperature					
Rb_2SnI_6	0.88	Cubic at 293°K	26		
(					
$(NH_4)_2TeBr_6$	0.90	Cubic above 168°K	27,28	13	
K_2ReBr_6	0.91	Cubic above 245°K	6,29	22,23	21
K_2SnCl_6	0.92	Cubic above 262°K	2		18
K_2SeBr_6	0.93	Cubic above 240°K	3	15	
$(NH_4)_2SnBr_6$	0.93	Cubic at 293°K	10	4	18
$(NH_4)_2TeCl_6$	0.96	Cubic above 77°K	30	13	
K_2ReCl_6	0.97	Cubic above 111°K	29,31	22,23	19
3. Crystals which are cubic at all temperatures					
K_2PtCl_6	0.98	Cubic	1	12	
Cs_2TeI_6	1.00	Cubic	32	13	
Cs_2TeBr_6	1.07	Cubic	28,5	13	

structure of potassium hexabromostannate (K_2SnBr_6) at room temperature, using single crystal x-ray diffraction techniques. With a radius ratio of 0.86, the structure falls about midway between that of K_2TeBr_6 (radius ratio = 0.83) and undistorted K_2PtCl_6 structure (radius ratio = 0.89). Brown[7] shows that the distortion proposed by Markstein and Nowotny in the case of K_2SnBr_6 is of the same type as that in K_2TeBr_6 but is only about half as great. The present work was undertaken to refine the structure and study the nature of distortion in K_2SnBr_6 at room temperature. In the present study, the single crystal intensity data have been used to determine the positional and thermal parameters of atoms in the crystal.

In refining the structure of K_2SnBr_6 at room temperature, we have found that it is monoclinic with the space group $P2_1/n$, thus having a symmetry lower than tetragonal and thus satisfying the Nuclear Quadrupole Resonance result. Further, we have found that the $SnBr_6^{=}$ ion has the configuration of a regular octahedron and there is no significant difference in the three non-equivalent Sn-Br distances and the angles do not vary significantly from 90°. The distortion in K_2SnBr_6 is found to be similar to that in K_2TeBr_6 as suspected.

Chapter 2

DEVELOPMENT OF X-RAY DIFFRACTION METHODS

The use of x-rays for investigating the structure of matter began with Von Laue's discovery of the diffraction of x-rays by crystals in 1912. A crystal consists of a basic unit of structure repeated regularly in a three dimensional array and it acts as a three dimensional grating with respect to x-rays. X-ray diffraction, therefore, led to the possibility of studying the arrangement of atoms inside a crystal. Consequently, several important fields of investigation opened up.

During the early stages of the development of x-ray crystallography, mostly inorganic substances were investigated because of the simplicity of their chemical composition. These included the structures of diamond and graphite, whose atomic arrangements were later found to be of fundamental importance to organic chemistry. Interest in more and more complex structures grew and the techniques gradually advanced. In 1915, W. H. Bragg pointed out that as the density of scattering matter in a crystal is periodic in three dimensions, it should be expressible as a summation of a three dimensional Fourier series, the terms of which

are derivable from the diffraction intensities from the various possible reflecting planes in the crystal. The main problem, therefore, was to measure the intensities of all possible reflections, so as to miss asfew of the terms as possible in the summation and to determine the phases of the terms, the magnitude alone being given by the diffraction intensities. Therefore the attention of the crystallographers was directed towards improved methods of recording and interpreting x-ray diffraction photographs. In 1924, Weissenberg introduced the idea of employing moving film methods of recording and indexing the diffraction pattern. In 1927, Bernal put forward the simplified method of interpreting rotation photographs based on Ewald's concept of reciprocal lattice. The determination of the phases of reflections remained a great hurdle in solving complex crystal structures. Usually, this is achieved by the well known trial and error method. However, valuable information can often be obtained from the available optical and magnetic data.

In 1934, Patterson showed that there exists a relationship between the inter-atomic vector distances and the intensity of the x-ray reflections. Instead of structure factors, he used the squares of structure amplitudes as Fourier coefficents and the resulting synthesis was related in a simple way to the crystal structure.

In recent times, with the development of computer

technology, there has been a great progress in the determination of crystal structures. As a result of the work of Astbury, Bernal, Perutz and many others, it has been possible to determine the structures of a large number of molecules of biological interest. Many such complicated structures have already been reported by different workers e.g. DNA by Watson and Crick (1951), ribonuclease by Harker and Kartha (1967), myoglobin by Kendrew et al (1958) and haemoglobin mainly by Perutz and his coworkers.

Crystallographers have also been trying to study the structures of small molecules in greater details. These include the determination of the exact mean positions of all atoms, a study of electron distribution of atoms in a state of rest and a knowledge of zero-point motion and thermal vibration of atoms.

Chapter 3

THEORY OF STRUCTURE DETERMINATION

3.1 Fundamentals of Crystallography

A systematic science of crystallography has been developed which serves as the basis for the rational interpretation of the x-ray diffraction data. The steps in the development of this information may be summarized as follows:

(a) A crystal has planar bounding faces and symmetry. It is essential to choose a system of coordinates in order to express the positions of these planes, relative to one another, in space. The planes are then indexed in terms of their intercepts upon the axes of a system of coordinates. An immense amount of experimentation has proved that all angle measurements and indexing of plane faces can be accounted for by seven systems of coordinates. In other words, there are seven crystal systems.

(b) As a result of further experience it is now certain that the indices of all the plane faces of the crystal are always small whole numbers.

(c) The symmetry of an object is an expression of the fact that the object has equal properties in different directions. The following symmetry operations are per-

formed to bring equivalent directions in space into coincidence.

Axes of symmetry: Points in crystal may have one-, two-, three-, four- or six-fold axes. This means that equivalent points may be brought into coincidence by a rotation of 360, 180, 120, 90 or 60 degrees.

Plane of symmetry (mirror operation): in which points on one side of a plane are mirror images of points on the other.

Centre of symmetry or combined 2-fold rotation and reflection across a plane perpendicular to the axis.

When these symmetry operations are combined in every possible way, using the seven crystal classes, it can be shown that there are 32 point groups which define 32 classes in terms of point symmetry. There are also "screw" axes of symmetry involving rotations about and translation along an axis and "glide" planes of symmetry in which a figure is brought into coincidence by reflection in a plane combined with translation of a definite length and direction in the plane. When these are combined with translational symmetry, the result is a total of 230 combinations of space groups. The definition of the symmetry of a crystal by its space group is unique.

3.2 Theory of x-ray diffraction by crystals

Like visible light, x-rays may be considered as an

electro-magnetic wave. The wavelengths of x-rays used in the determination of crystal structures vary between 0.5 and 3 A. Any electron in the path of an x-ray scatters it. An atom consists of electrons around a positively charged nucleus. The nucleus, because of its large mass, can be neglected when we consider the scattering of x-rays. Each electron in the atom scatters x-rays. Therefore, the atom as a whole scatters x-rays to an extent dependent on the number of electrons in the atom, i.e., dependent on the atomic number. Because of the regular arrangement of atoms in the crystal the scattered x-rays interfere to form a diffraction pattern.

Laue diffraction equations illustrate effectively the conditions for the formation of a diffracted beam. P_1 and P_2 are two lattice points separated by a vector $\underline{r}$ (See Fig. 2), $\underline{s_o}$ is the unit incident wave vector and $\underline{s}$ is the unit scattered wave vector. P_2A and P_1B are the projections of $\underline{r}$ on the incident and scattered wave directions. The path difference between the two scattered waves from P_1 and P_2 is

$$P_2A - P_1B = \underline{r}\cdot\underline{s_o} - \underline{r}\cdot\underline{s}$$
$$= \underline{r}\cdot(\underline{s_o} - \underline{s})$$
$$= \underline{r}\cdot\underline{S} \text{ where } S = \underline{s_o} - \underline{s}$$

If 2θ is the angle that $\underline{s}$ makes with $\underline{s_o}$, then $|\underline{s_o} - \underline{s}| = 2\sin\theta$) since $\underline{s_o}$ and $\underline{s}$ are unit vectors (See Fig. 3).

The phase difference φ is $\left(\frac{2\pi}{\lambda}\right)$ times the path difference. Therefore

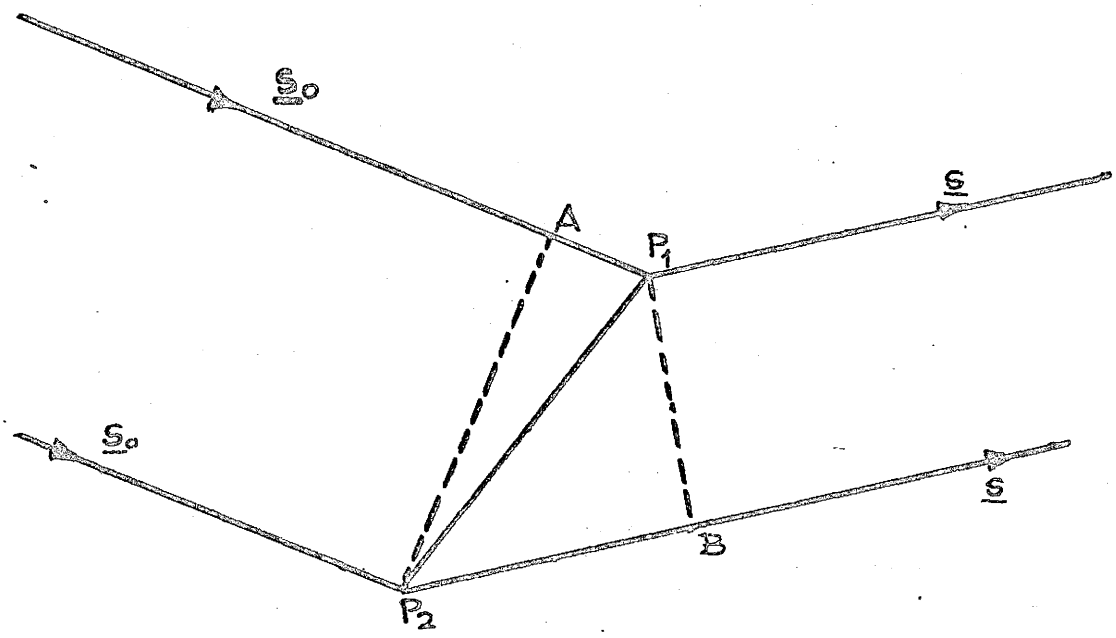

Fig. 2. Scattering of x-rays by Scatterers situated at two lattice points.

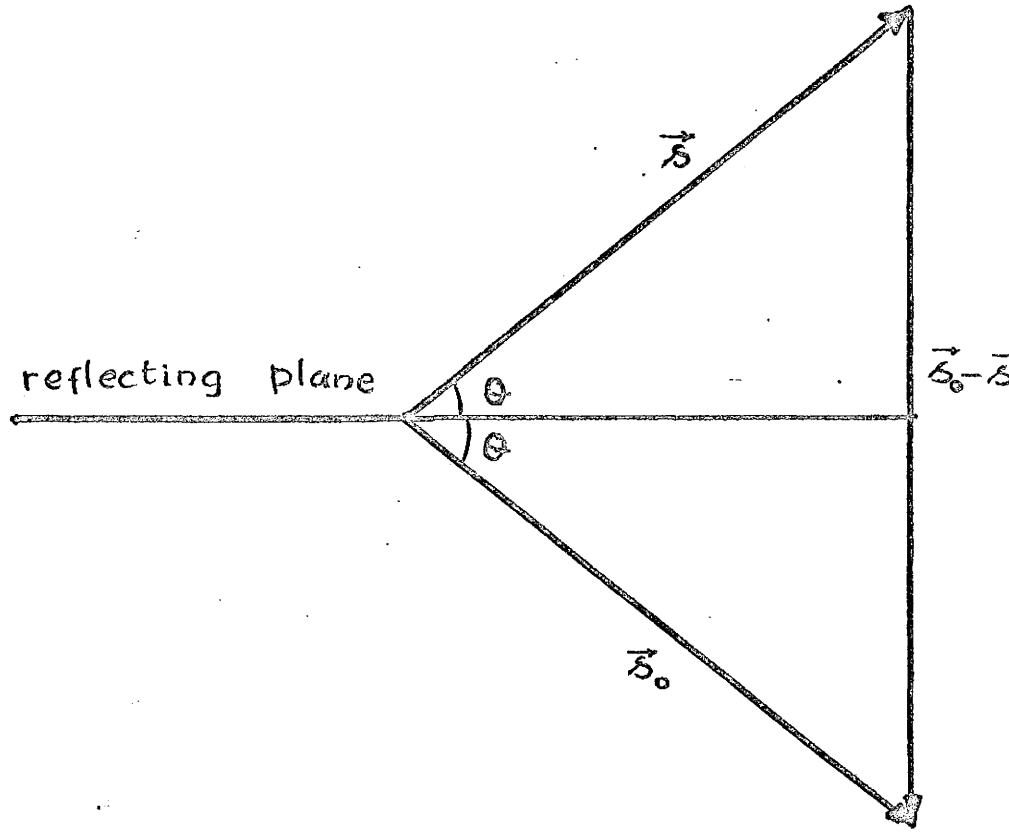

Fig. 3. Relationship between the vectors $\underline{s}_o$, $\underline{s}$ and S

$$\varphi = \frac{2\pi}{\lambda} (\underline{r} \cdot \underline{S})$$

The amplitude of the scattered wave is a maximum in a direction such that the contribution from each lattice point differs in phase only by an integral multiple of 2π. Therefore, for diffraction maxima,

$$\varphi = \frac{2\pi}{\lambda} (\underline{r} \cdot \underline{S}) = 2\pi n$$

where n is an integer

$$\therefore \quad \underline{r} \cdot \underline{S} = n\lambda$$

If $\underline{a}$, $\underline{b}$, $\underline{c}$ are the primitive translation vectors, the vector $\underline{r}$ can be specified as

$$\underline{r} = m_1\underline{a} + m_2\underline{b} + m_3\underline{c}$$

where m_1, m_2 and m_3 are integers. Thus

$$\underline{r}\cdot\underline{S} = m_1\underline{a}\cdot\underline{S} + m_2\underline{b}\cdot\underline{S} + m_3\underline{c}\cdot\underline{S} = n\lambda$$

Since m_1, m_2 and m_3 are independent, each of them must be equal to an integer. That is,

$$\underline{a}\cdot\underline{S} = h\lambda$$

$$\underline{b}\cdot\underline{S} = k\lambda$$

$$\underline{c}\cdot\underline{S} = l\lambda$$

where h, k, l are integers. These are the LAUE EQUATIONS.

If α, β, γ are the direction cosines of $\underline{S}$ with respect of $\underline{a}$, $\underline{b}$, $\underline{c}$, then

$$\underline{a}\cdot\underline{S} = h\lambda = 2a\alpha\sin\theta$$

$$\underline{b}\cdot\underline{S} = k\lambda = 2b\beta\sin\theta$$

$$\underline{c}\cdot\underline{S} = l\lambda = 2c\gamma\sin\theta$$

The vector $\underline{S}$ has got a special significance. $\underline{S}$ is perpendicular to the crystal planes of which h, k, ℓ are Miller indices.

If $d(hk\ell)$ is the spacing between two adjacent planes of a set $(hk\ell)$, the

$$d(hk\ell) = \frac{a\alpha}{h} = \frac{b\beta}{k} = \frac{c\gamma}{\ell} = \frac{\lambda}{2\sin\theta} .$$

Therefore, $2d \sin\theta = \lambda$.

It is also implicit that both $\underline{s}_o$ and $\underline{s}$ make an angle with this plane.

The equations $2d\sin\theta = \lambda$ is nothing but the well known Bragg law, which states that diffracted beams are found only for special cases satisfying the above condition. This results from the fundamental periodicity of the structure and does not refer to the actual arrangement of atoms in the lattice. An important consequence of the law is that the wave lengths must be less than 2d if Bragg reflection is to occur.

The conditions for an x-ray beam to be diffracted may be expressed with the help of the reciprocal lattice which is widely used in crystallography.

The reciprocal lattice primitive translation vectors $\underline{a}^*$, $\underline{b}^*$, $\underline{c}^*$ are defined by

$$\underline{a}^* . \underline{a} = \underline{b}^* . \underline{b} = \underline{c}^* . \underline{c} = 1$$

$$(\underline{a}^* . \underline{b}) = (\underline{a}^* . \underline{c}) = 0$$

$$(\underline{b}^* . \underline{c}) = (\underline{b}^* . \underline{a}) = 0$$

$(\underline{c}^*.\underline{a}) = (\underline{c}^*.\underline{b}) = 0$

The reciprocal lattice has a definite orientation relative to the crystal lattice. Every point in the reciprocal lattice corresponds to a possible reflection from the crystal lattice.

The Bragg equations has a simple geometrical significance in reciprocal lattice. AO is a vector of length $(1/\lambda)$ in the direction of incident radiation (see Fig. 4), terminating at the origin of reciprocal lattice. If we draw a sphere of radius $(1/\lambda)$ with A as centre, then the possible directions of the diffracted rays for this incident ray are determined by the intersections of the sphere with the points of the reciprocal lattice. The direction AB is a direction of a diffraction maximum and B is a point of the reciprocal lattice. This is Ewald's construction.

We can now prove the Ewald constructions. Let $\underline{S} = j\underline{a}^* + m\underline{b}^* + n\underline{c}^*$, where j, m and n are any (non-integral) numbers having dimensions of length (since $\underline{S}$ is dimensionless).

Then the Laue equations reduce to

$$\underline{a}.j\underline{a}^* + \underline{a}.m\underline{b}^* + \underline{a}.n\underline{c}^* = h\lambda$$

$$\underline{b}.j\underline{a}^* + \underline{b}.m\underline{b}^* + \underline{b}.n\underline{c}^* = k\lambda$$

$$\underline{c}.j\underline{a}^* + \underline{c}.m\underline{b}^* + \underline{c}.n\underline{c}^* = l\lambda$$

i.e.

$$j\underline{a}.\underline{a}^* = h\lambda$$

$$m\underline{b}.\underline{b}^* = k\lambda$$

$$n\underline{c}.\underline{c}^* = l\lambda$$

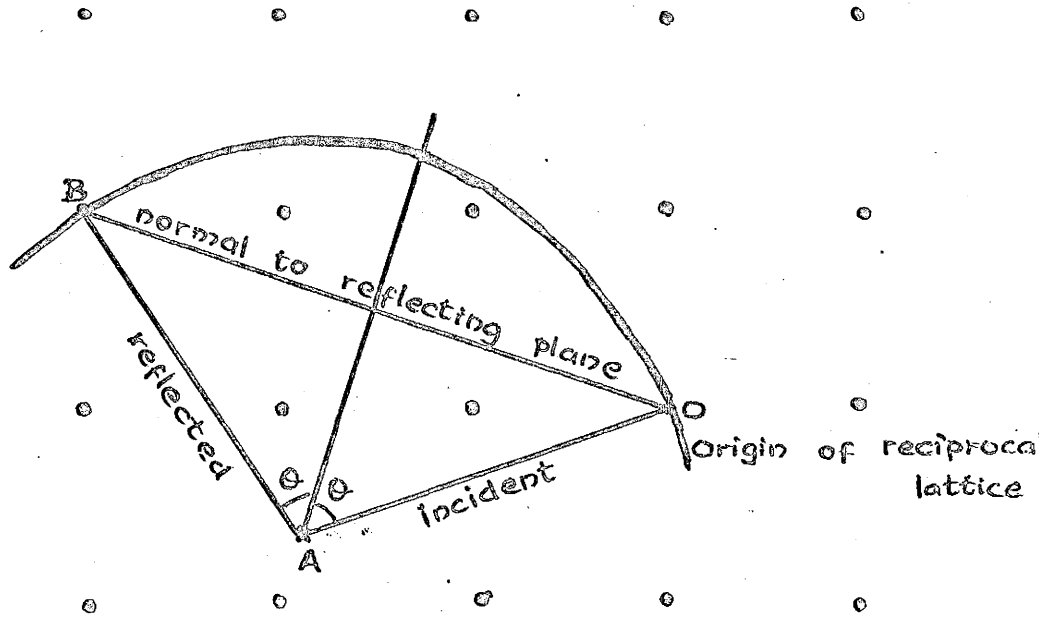

Fig. 4. Ewald's construction of reciprocal lattice

or $j = h\lambda$

$m = k\lambda$

$n = \ell\lambda$

Therefore, $\underline{S} = h\lambda\underline{a}^* + k\lambda\underline{b}^* + \ell\lambda\underline{c}^*$

$$\text{or } \frac{1}{\lambda}\underline{S} = h\underline{a}^* + k\underline{b}^* + \ell\underline{c}^*$$

In Fig. 4, B is a lattice point in reciprocal space.

$$OB = h\underline{a}^* + k\underline{b}^* + \ell\underline{c}^*$$

$$= \frac{1}{\lambda}\underline{S} = \frac{2\sin\theta}{\lambda} ,$$

But $OB = 2AO \sin\theta'$ where θ' is the angle shown as θ in Fig. 4.

Therefore,

$$OB = 2AO \sin\theta' = \frac{2\sin\theta'}{\lambda}$$

Thus $\underline{\underline{\theta' = \theta}}$

3.3 Intensities of reflections

The intensities of reflections are used to determine the positions of atoms within the unit cell. The structure factor $F(hk\ell)$ of a reflection is given by the Fourier transform of the electron density $\rho(xyz)$ within the cell as[33]

$$F(hk\ell) = V\int_{x}\int_{y}\int_{z=0}^{1} \rho(xyz)\, \exp\left[2\pi i\,(hx+ky+\ell z)\right] dx\,dy\,dz$$

where V denotes the volume of the unit cell, and x, y and z are the fractional coordinates of the volume element ($\underline{V}$ dxdydz) considered.

F(hkl), as will be seen in the next chapter, is a complex quantity and is related to the observed intensity

I of the diffracted beam by the expression $I \propto |F(hkl)|^2$. Thus from the measurement of intensities, the moduli of the structure factors can be evaluated and these can be used in the determination of the crystal structure.

The pattern which results from the diffraction of a crystal is normally recorded on films. The diffraction maxima appear as spots of varying intensity on the film. However, one is faced with certain difficulties in the measurement of these intensities. Corrections have to be made for variation in the size and shape of the spots, non-uniform distribution of intensity over the spots and the presence of different background around the spots found in different areas on the film.

In a real crystal, due to imperfection, adjacent volume units are not exactly parallel. Therefore, the crystal must be turned slightly in order to bring each unit into the Bragg condition for reflections to occur. This results in the spreading of the spot over a small range. Thus the peak intensity of a reflection does not necessarily give a reliable measure of the structure amplitude. A better measure can be obtained by summing the energy reflected by a set of planes as the sample is rotated through small angles close to the Bragg angle, i.e. by integrating the intensities.

James[34] has deduced an expression for the integrated intensity. The crystal is assumed so small that the absorption within it may be neglected. It is assumed to rotate

with uniform angular velocity ω about an axis parallel to a set of planes and through a range of angles. The energy E reflected by the crystal is proportional to the volume Δv of the crystal. For the case of unpolarised incident radiation

$$\frac{E\omega}{I_o} = Q\,\Delta v$$

where I_o is the energy incident per unit area in the beam and

$$Q = \frac{N^2\lambda^3}{\sin 2\theta}|F|^2\left(\frac{e^2}{mc^2}\right)^2 \frac{1+\cos^2 2\theta}{2}$$

where $|F|$ is the structure amplitude, θ is the Bragg angle and N is the number of unit cells in the volume of the crystal. The quantity $(E\omega/I_o)$ is called "Integrated reflection" from the crystal element.

The factor $\frac{1+\cos^2 2\theta}{2}$ is called the "Polarisation factor p", which is the amount by which the intensity of the diffracted beam is reduced owing to partial polarisation on diffraction. The factor $(1/\sin 2\theta)$ is known as the "Lorentz factor" which is proportional to the time the crystal takes to pass through a reflecting position. This factor varies both with the Bragg angle and with the particular arrangement by which the diffraction pattern is recorded. The correction for Lorentz and polarisation effects is usually applied in the combined form. The observed structure amplitude $|F|$ of a reflection is evaluated from its measured intensity I using the relation

$$|F| = K\left(\frac{I}{Lp}\right)^{\frac{1}{2}}$$

where K is a constant dependent on the wavelength and crystal size and is initially taken arbitrarily as one.

3.4 Extinction

This is one of a number of physical factors affecting the intensities, others being absorption and temperature motion of the atoms. In general, it is not uncommon to assume that some of these effects are so small that they can be neglected.

In deriving the relation between the intensity and square of scattering amplitude, it is assumed that the crystal consists of a small volume element. This eliminates any concern for absorption and "extinction". Extinction is a phenomenon which results in the attenuation of the primary beam of x-rays when the crystal is in a diffracting position. Therefore it reduces the intensity of the diffracted beam particularly for strong reflections. This effect is very difficult to correct for experimentally because it depends on the physical perfection of the crystal. For this reason, it is ordinarily ignored in many crystal structure analyses.

3.5 Absorption

X-rays are absorbed by matter. The extent to which

this occurs in the tiny crystals used in structure analysis is normally great and therefore, the effects of absorption cannot be neglected in accurate work. The amount of absorption in the crystal is difficult to calculate as it depends on the shape of the sample and also on the relation of the direct and the diffracted beams to this shape. It is always possible to approximate the allowance.

If we consider an infinite plate shaped crystal of uniform thickness t, mounted on a precession camera such that the x-ray beam is incident on the largest face of the crystal, the absorption factor A for zero-layer reflections is given by

$$A = \frac{I}{I_o} = \exp.\ (-\mu t \sec\bar{\mu})$$

where $\bar{\mu}$ is the precession angle and μ is the absorption coefficient.[35] For small plate shaped crystals immersed in the incident beam the path lengths of the rays are all equal except for the rays incident on the region close to the edges of the crystal. Thus the absorption can be considered uniform for all reflections on the same layer, if the edge effect is neglected. For relatively thicker plate shaped crystals, the edge effect is significant as the absorption can be considered uniform only over a small region near the centre. For cube shaped crystals which can be approximated by a sphere, edge effect is important. For a spherical crystal, the absorption correction varies with

the Bragg angle.[36] For crystals with $\mu R < 2$, the ratio of the absorption factor A for $\theta = 0^\circ$ to that for $\theta = 30^\circ$ is less than 1.5.

3.6 Structure factor

A crystal can be represented by placing a certain arrangement of atoms within each unit cell of the lattice. If the unit cell of a crystal contains N atoms at points x_n, y_n, z_n which can be considered as the coordinates with respect to the axes of the lattice, then the position of the nth atom in the unit cell can be represented by

$$\underline{r}_n = x_n\underline{a} + y_n\underline{b} + z_n\underline{c}$$

The path difference between the waves scattered by these atoms and those that would be scattered by a set of atoms at the points of the lattice that define the origins of unit cells is $\underline{r}_n \cdot \underline{S}$. Then the expression for the complete wave scattered by the nth lattice contains a term

$$f_n \exp\left[\left(\frac{2\pi i}{\lambda}\right)\underline{r}_n \cdot \underline{S}\right]$$

or $$f_n \exp\left[2\pi i \ \frac{\underline{r}_n \cdot \underline{S}}{\lambda}\right]$$

where f_n is the scattering factor of nth atom. Thus the expression for the complete wave scattered by the crystal is

$$F = \sum_{n=1}^{N} f_n \exp\left[2\pi i \ \frac{\underline{r}_n \cdot \underline{S}}{\lambda}\right]$$

$$= \sum_{n=1}^{N} f_n \exp\left[2\pi i \ \frac{x_n\underline{a}\cdot\underline{S}}{\lambda} + \frac{y_n\underline{b}\cdot\underline{S}}{\lambda} + z_n\frac{\underline{c}\cdot\underline{S}}{\lambda}\right]$$

We have $\underline{a}\cdot\underline{S} = h\lambda$ (from Laue equations).

Therefore,

$$x\,\frac{\underline{a}\cdot\underline{S}}{\lambda} = hx$$

$$y\,\frac{\underline{b}\cdot\underline{S}}{\lambda} = ky$$

$$z\,\frac{\underline{c}\cdot\underline{S}}{\lambda} = lz$$

Thus,

$$F = \sum_{n=1}^{N} f_n \exp. 2\pi i \left(hx_n + ky_b + lz_n\right).$$

The expression for the structure factor as written above is a complex quantity. This means that the phase of the scattered wave is not simply related to that of the incident wave. The phase is not an observable quantity. The only quantity that is observable is the intensity which is proportional to the square of the scattering amplitude. If $F = A + iB$ where

$$A = \sum_{n}^{} f_n \cos 2\pi \left(hx_n + ky_n + lz_n\right)$$

$$B = \sum_{n}^{} f_n \sin 2\pi \left(hx_n + ky_n + lz_n\right)$$

where f_n is the scattering factor for the nth atom, then $F^2 = A^2 + B^2$. These are the equations that are used in practice.

If the structure is centro-symmetric, then for each atom at (x, y, z) in the unit cell, there is a corresponding atom at $(\bar{x}, \bar{y}, \bar{z})$. Then the contribution of this pair

to F is given by,

$$f\left[\cos 2\pi(hx+ky+lz) + i \sin 2\pi(hx+ky+lz) + \cos 2\pi(hx+ky+lz) - i \sin 2\pi(hx+ky+lz)\right] = 2f \cos 2\pi(hx+ky+lz).$$

Hence,

$$F = 2 \sum_{n=1}^{(N/2)}{}' f_n \cos 2\pi(hx_n + ky_n + lz_n)$$

where the summation is carried out only over half the number of atoms in the unit cell. In this case, the structure factor is real and the phase is reduced to the two possibilities that F is positive or negative.

3.7 Atomic scattering factor

So far the electrons in the atoms have been assumed to be the scattering units. If there are Z electrons in an atom, then the amplitude of the beam scattered by the atom is Z times the amplitude of the beam scattered by an individual electron. The linear dimensions of the electrons have so far been neglected in comparison with the space lattice dimensions and also with the wavelengths of x-rays. In atoms, the electrons occupy a finite volume. The phase differences between rays scattered from different points have to be taken into account. These phase differences are small for small angles of diffraction but become larger for greater angles of diffraction.

For small angles, the amplitude of scattering

by an atom can be considered as the sum of amplitudes of scattering by individual electrons. For large angles, the phase difference is large and the scattered beam becomes weaker, i.e. the factor becomes less than Z. This factor is called the "Atomic Scattering Factor f" and values based on various methods of calculation are tabulated in the International Tables.

3.8 Temperature factor

At any temperature, the atoms oscillate with a finite amplitude. The frequency of this oscillation (about 10^{13} per second) is much smaller than the frequency of x-rays (10^{18} per second). Therefore, to a beam of x-rays, the atoms would appear to be stationary but slightly displaced from their mean positions. Thus, atoms in the neighbouring cells, which should scatter in phase will scatter slightly out of phase. The total effect of this will be to reduce the scattering factor of the atom.

If f_o is the scattering factor of an atom at rest, then the scattering factor that is used in practice is

$$f_o \exp \frac{-B\sin^2\theta}{\lambda^2}$$

where θ is the Bragg angle and B is a constant called the Debye-Waller Temperature factor. The value of B can be evaluated in terms of the Debye characteristic temperature

$$B = \frac{6h^2T}{mk\Theta^2}\phi\left(\frac{\Theta}{T}\right)$$

where m : mass of the atom

h : Planck's constant

k : Boltzmann constant

T : Absolute temperature

θ : Debye characteristic temperature

and $Q(\theta/T)$ is a quantization factor which has been tabulated and does not differ appreciably from unity unless $(\theta/T) < 1$.

In general, the vibrations of the atoms will be anisotropic and of different amplitudes in different directions. The effective scattering factor can then be given by

$$f = f_o \exp. -(\beta_{11}h^2 + \beta_{22}k^2 + \beta_{33}l^2 + 2\beta_{12}hk + 2\beta_{23}kl + 2\beta_{13}hl).$$

where f_o is the scattering factor of the atom at rest and β's are the coefficients of the anisotropic temperature factor.

Chapter 4

EXPERIMENTAL PROCEDURES

4.1 Measurement of Intensity

To estimate the intensity of a reflection spot on the film visually, one carries out a comparison of the spot with one of a series of spots prepared by photographing one particular reflection at different known exposure times. The peak intensity of a reflection is measured in this way. In visual estimation of intensities, it is assumed that the peak intensity is proportional to the integrated intensity. In fact, this is not so frequently because of the non-uniformity in the size of the spots.

To integrate the intensities, the cross sections of the reflections should be taken into account, since one has to sum the intensity from all parts of the spot. This is achieved by recording the reflection on a film which is moved over a series of regular small intervals so that the density of blackening at the centre of the spot on the film attains a constant value which measures the integrated intensity of a reflection.[35]

A mechanical device for recording the integrated

intensity on the Buerger Precession Camera has been described by Nordman et al.[38] A microdensitometer can be used to measure the integrated intensities of reflections. The densitometer traces of the spots will show plateau like profiles whose heights, corrected for the background, are proportional to the integrated intensities.

From the measured intensities, the structure amplitudes can be evaluated and these can be used to determine a trial model for the structure using either the Patterson function or the so-called direct methods. Alternatively a trial model may be proposed from chemical or packing considerations.

4.2 Refinement

Once a model of the structure has been proposed, it is necessary to improve the preliminary coordinates by a process of refinement. The structure amplitudes can be evaluated from the observed intensities. The necessary condition for a proposed structure to be correct is that the calculated structure factors should agree well with the observed structure factors. It is common to measure this agreement by a "Residual" of the form

$$R = \frac{\sum |F_o| - |F_c|}{\sum |F_o|}$$

where the numerator is the sum of all the differences between the observed and calculated structure factors and

the denominator is the sum of all the observed structure factors. Thus R is a measure of the relative discrepancies of the structure factors for the model. The value of R is a comparatively small fraction when the structure is correct. Correct structures usually have $R<0.25$ and very well refined structures may have R in the neighbourhood of 0.05.

The value of R deduced for any model depends on how the observed structure amplitudes with very small values are treated. On a photographic film, there is a lower limit below which $|F_o|$ cannot be observed. For such unobserved reflections, the value of the least observed intensity with a large error is assigned.

With modern computing facilities, the structure can be refined by the method of least squares described below. By this method, it is possible to refine simultaneously all the parameters of the atoms in the asymmetric unit using three dimensional intensity data.

4.3 Method of Least Squares

The observed structure factors are subject to errors of observation so that the refinement consists in finding the model which yields the most acceptable fit between the calculated structure factors and the observed structure factors. Legendre proposed that the most acceptable values of variables were such as to make the sum of the squares of

the errors a minimum.

Suppose an observable quantity q is a linear function of set of variables x, y, z

i.e. $q = ax + by + cz + \ldots$ (1)

Suppose there are different errors of observation E associated with each q.

Therefore, $q + E = ax + by + cz + \ldots$ (2)

The error in each observation $E = ax + by + cz + \ldots - q$. According to the Legendre principle, $\sum_j E_j^2$ should be made a minimum, where j runs from 1 to m where m is the number of observations.

$$\sum_j E_j^2 = \sum_j (a_j x + b_j y + c_j z + \ldots - q_j)^2. \quad (3)$$

is a minimum when its partial derivatives with respect to x, y, z .... vanish, i.e.

$$\frac{\partial \sum_j E_j^2}{\partial x} = 2\sum_j (a_j x + b_j y + c_j z + \ldots - q_j)\, a_j = 0$$

$$\frac{\partial \sum_j E_j^2}{\partial y} = 2\sum_j (a_j x + b_j y + c_j z + \ldots - q_j)\, b_j = 0$$

etc. (4)

These can be written as

$$(\Sigma' a_j^2)x + (\Sigma' a_j b_j)y + \ldots = \Sigma' a_j q_j$$

$$(\Sigma' b_j a_j)x + (\Sigma' b_j^2)\, y + \ldots = \Sigma' b_j q_j$$

etc. (5)

These equations, known as "Normal Equations" are n equations

in n unknowns, where n is the number of variables. From these, values of x, y, z ... which best satisfy Legendre principle can be determined.

In making observations like (1), some observations may be considered more trustworthy than others. The various observations q_j may be assigned weights w_j, which indicate relative estimates of their reliabilities. Therefore both sides of (2) are multiplied by w_j. When followed through, this replaces each quantity in (5) by its product with w_j.

This method can be applied to find the values of the coordinates of the atoms in the structure which best fit the observed structure factors. Each structure factor is computed from

$$F_c = \sum_r f_r \exp.\left[2\pi i \left(hx_r + ky_r + \ell z_r\right)\right]$$

Here the variables are the exponential in x, y and z and are not in the form of the desired linear equations. Linear relations, however, can be devised by using the first two terms in Taylor's series. In this application, the above function f is treated as follows.

If each of the parameters x, y, z defining the proposed structure is assumed to have an error ε_x, ε_y, ε_z, then,

$$f(x + \varepsilon_x, y + \varepsilon_y, z + \varepsilon_z) = f(xyz) + \varepsilon_x \frac{\partial f(xyz)}{\partial x} +$$

$$+ \varepsilon_y \frac{\partial f(xyz)}{\partial y} + \varepsilon_z \frac{\partial f(xyz)}{\partial z}$$

If $f(x + \varepsilon_x, y + \varepsilon_y, z + \varepsilon_z) = F_o$

$f(xyz) = F_c$.

then $\Delta F = F_o - F_c$ and from Taylor expansion

$$\Delta F = F_c + \sum_r \left(\varepsilon_{xr} \frac{\partial F_c}{\partial xr} + \varepsilon_{yr} \frac{\partial F_c}{\partial yr} + \varepsilon_{zr} \frac{\partial F_c}{\partial zr} \right) - F_c$$

$$= \sum_r \varepsilon_{xr} \frac{\partial F_c}{\partial xr} + \varepsilon_{yr} \frac{\partial F_c}{\partial yr} + \varepsilon_{zr} \frac{\partial F_c}{\partial zr} \qquad (6)$$

This summation extends over all the atoms in the structure. For each observed reflection there exists such an equation. When the observational error, E, is added to each equations like (6), the set of equations can be recast in the form

$$\varepsilon_j = a_j x + b_j y + c_j z + \ldots . - q_j .$$

from which the normal equations like (5) can be derived.

The solutions reduce to

$$\varepsilon_{xr} = \frac{\sum_{i=1}^{m} w_i \left(\frac{\partial F_i}{\partial x} \right)_r \Delta F}{\sum_{i=1}^{m} w_i \left(\frac{\partial F_i}{\partial x} \right)_r^2}$$

Where w_i is a weighting factor and m is the total number of reflections.

When a weighting function, w, is used, the least squares refinement minimizes $\sum w(|F_o| - |F_c|)^2$. Each weight w is taken as the inverse of the square of the standard deviation of the corresponding observation.

The weighted R-factor is given by

$$R_2 = \left\{ \frac{\sum w_i \; (|F_o| - |F_c|)_i^2}{\sum w_i \; (|F_o|)^2} \right\}^{1/2} .$$

Chapter 5

EXPERIMENTAL WORK

Potassium hexabromostannate (K_2SnBr_6) was prepared by adding potassium bromide to the solution of tin (IV) tetrabromide in hydrobromic acid containing a small amount of bromine.[39] The crystals thus prepared were recrystallised from the mixture of dilute hydrobromic acid and a small quantity of bromine.

These crystals were found to decompose in very humid air and therefore they had to be sealed in dry capillary tubes during the experiments.

The density of the crystal was calculated using the formula

$$\text{Density } (gm/cm^3) = \frac{Z \times \text{Formula Weight (amu)} \times 1.660 \times 10^{-24}}{\text{Volume of unit cell } (\text{Å}^3) \times 10^{-24}}$$

Knowing the density, the linear absorption coefficient μ both for Cu K_α and Mo K_α radiation could be calculated, from the mass absorption coefficients listed in the International Tables.[36]

For single crystal x-ray dffraction work, the major consideration which limits the size of the crystal is the

absorption of x-rays by the crystal. If the absorption coefficient is large, the relation $F^2 = KI/L_p$ breaks down and this limits the size of the crystal.

In order to avoid the absorption correction, the size of the crystal to be used for x-ray diffraction work was calculated, assuming the crystal to be spherical in shape, taking $\mu R \sim 1$ where R is the radius of the sphere.

The values of μ calculated are as follows:

Cu K_α radiation : 497.3 cm^{-1}

Mo K_α radiation : 240.4 cm^{-1}

The maximum sizes of the crystal permissible were:

Cu K_α radiation : 0.02 mm radius

Mo K_α radiation : 0.04 mm radius

Because of low absorption of Mo K_α radiation as compared to the Cu K_α radiation, Mo radiation is preferred. Its smaller wavelength allows a greater number of reflections to be recorded. This becomes particularly important when the data are being collected on a precession camera which only records the diffraction pattern out to a Bragg angle of 30°.

Several crystals were picked from the sample and examined under a polarising microscope to check whether they were single crystals or not. Then a crystal which appeared to have well developed faces and also which seemed to be a single crystal, was sealed in a dry capillary tube and mounted on a goniometer head. The crystal chosen had

the dimensions: 0.021 x 0.011 x 0.005 cm.

The crystal along with the goniometer head was mounted on a Supper Integrated Precession Camera with the face (112) of the crystal along the goniometer axis perpendicular to the direction of the incident beam. The unintegrated photograph of zero layer was first taken.

The cell dimensions were measured from the films making use of high angle reflections and were found to be:

$\underline{a}$ = 7.435 ± 0.017 Å

$\underline{b}$ = 7.437 ± 0.017 Å

$\underline{c}$ = 10.568 ± 0.006 Å.

Those of Markstein and Nowotny[10] for the pseudo-cubic cell were $\underline{a}$ = 7.43 Å and $\underline{c}$ = 10.61 Å and those of Galloni et al[11] for the tetragonal cell were $\underline{a}$ = $\underline{b}$ = 10.520 Å and $\underline{c}$ = 10.624 Å.

The films were studied carefully. Initially a tetragonal space group $P4_12$ was assigned. This needs certain atoms to be placed in special positions. When this is done, it gives rise to two possibilities viz either the octahedron is not regular or the space group may be wrong. Since there was no reason to believe that the octahedron is irregular, another space group was tried. Further, as mentioned earlier, the NQR splitting of resonance lines indicated that the true symmetry is lower than tetragonal. Therefore a monoclinic space group $P2_1/n$ was assigned from the study of systematic absences. The systematic absences

TABLE H

Crystal data for K_2SnBr_6

		Markstein & Nowotny	Galloni et al	Present Work
System		Tetragonal	Tetragonal	Monoclinic
Space Group		P_{42_12}	P_{42_12}	P_{2_1}/n
Cell Constants	a =	7.430 Å	7.430 Å	7.435 ± 0.017
	b =	7.430 Å	7.441 Å	7.437 ± 0.017
	c =	10.61 Å	10.624 Å	10.568 ± 0.006
	β =	90°	90°	89° 50' ± 4'

were:

$ho\ell$: $h+\ell = 2n+1$

oko : $k = 2n+1$

Integrated photographs were taken for zero layer and three parallel layers and also for the zero layer perpendicular to these. Each layer was photographed with three different exposures: 2x, 6x and 18x the integrating cycles of 2 hours and 24 minutes. These photographs were indexed and the integrated intensities were measured using an automatic recording microdensitometer model MK IIIc of Joyce, Loebl and Co.

The standard errors in the observed structure amplitudes were calculated from an estimate which had been made of the standard errors of intensities. In assigning the errors to the measured intensities, due care was taken to see that each spot was treated according to its merit. For the unobserved reflections, the value of the intensity given was the least observed value on the film but a large standard error was assigned.

Then the observed intensities of the reflections were corrected for the Lorentz and Polarisation effects using PRELP - a program on CDC-6400 written for this purpose. This was used to obtain the observed structure amplitudes from the measured intensities.

Since the structure of K_2SnBr_6 was suspected of being similar to that of K_2TeBr_6, the latter was taken

Some typical densitometer traces

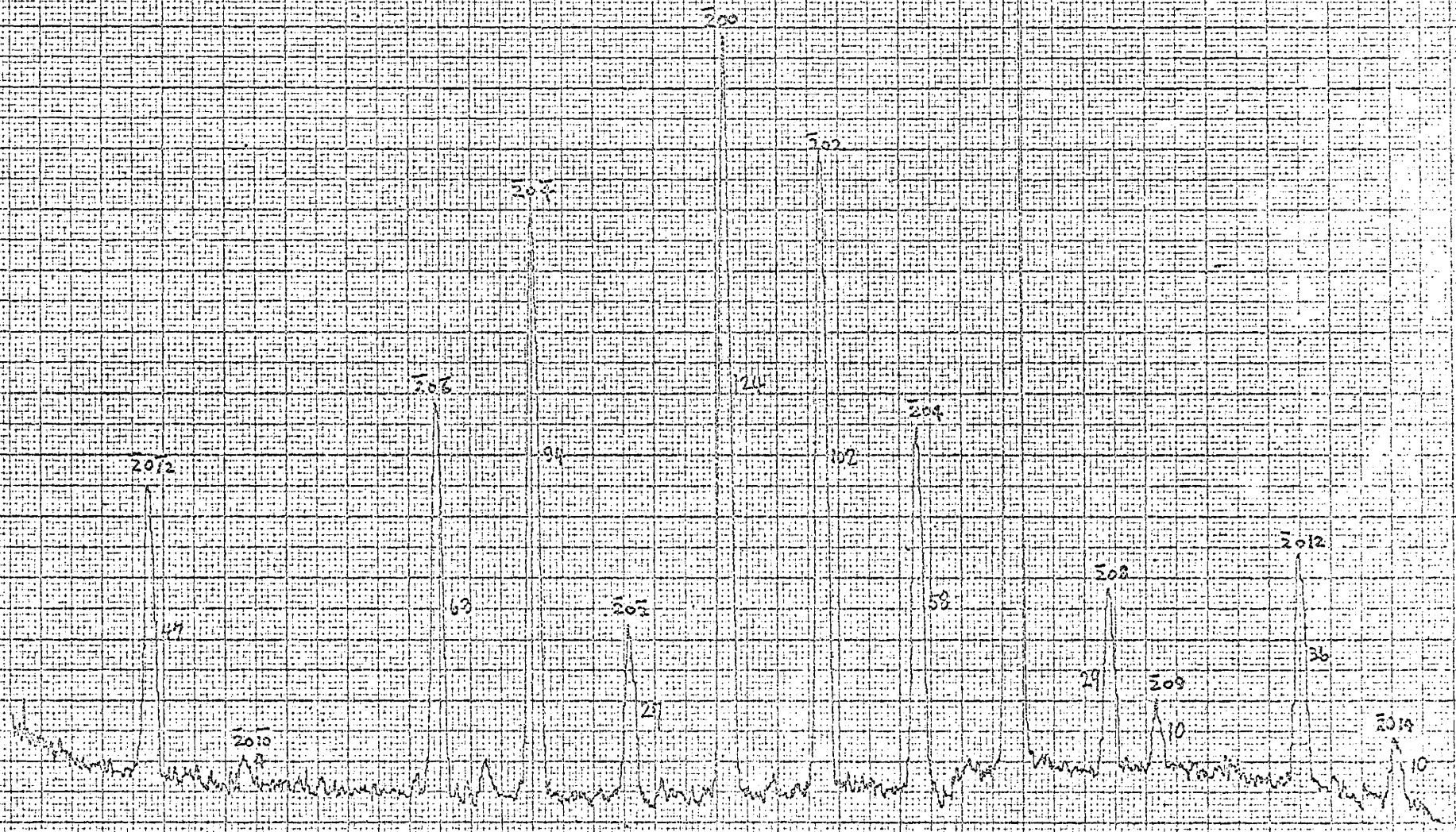

as a trial structure. The positions of the atoms for this model were: Sn at (0, 0, 0); the three bromine atoms at (0.0555, 0.0022, -0.2473); (0.2875, -0.2082, 0.0321); (0.2057, 0.2889, 0.0252); respectively and K at (0.012, -0.457, 0.250). At first only the isotropic temperature factor was assigned and the trial parameters were refined by a full matrix least square analysis of the three dimensional intensity data using the IBM-7040 program MACLS written in this laboratory by Stephens. This program makes use of a special sub-routine which calculates the structure factors and their derivatives for the particular space group or the problem for which it is being used.

A special sub-routine was prepared for the space group $P2_{1/n}$. The scattering curves required for this program were taken from the International Tables of x-ray Crystallography.[36] The variable parameters included in this program were the scale constants applied to the observed structure factors from layers photographed separately, the positional coordinates and the temperature factor of each atom.

Then the isotropic temperature factors were converted into anisotropic temperature factors and the refinement continued for four cycles after which no significant changes in the variable parameters were observed. In trying to refine the anisotropic temperature factors, the coefficients β_{12} and β_{23} for the tin atom had to be left equal to ze

since attempts to refine these two components gave ridiculously large numbers. The tin atom is in a centrosymmetric position and as such there should not be any restrictions on any of the components of the thermal ellipsoid for this atom. If a tetragonal space group had been assigned, then both β_{12} and β_{23} would have been identically equal to zero. As we have seen, the deviation from the tetragonal structure is not large. Therefore probably as far as tin is concerned, the structure is tetragonal and this accounts for the two coefficients β_{12} and β_{23} to be made zero.

The agreement, between the observed and calculated structure factors were checked after each cycle of refinement from the R-value. The final R factor was 0.116. The atomic parameters derived from the final cycle of refinement are listed in the Table B. The observed and calculated structure factors are given in Table C.

The interatomic distances and bond angles were calculated making use of a program MOLG written for IBM-7040 by Brown and Holder of this laboratory. This program diagonalises the thermal vibration tensor to give the RMS displacements of atoms along the three principal vibration axes. It also prints the direction cosines and angles made by these axes with the real and reciprocal crystal axes. It further calculates interatomic distances from each atom to any neighbouring atom out to a specified distance.

TABLE B

Atomic parameters derived from the final least squares Refinement

Atom	Position Coordinates			Standard Error Å	Temperature Factor					
	x/a	y/b	z/c		β_{11}	β_{22}	β_{33}	β_{12}	β_{13}	β_{23}
Sn	0	0	0	-	0.42	0.44	0.27	0	-0.03	0
Br(1)	0.0425	-0.0207	-0.2413		1.62	0.79	0.28	0.29	0.11	-0.09
Br(2)	0.2774	-0.2085	0.0251	0.001	0.82	0.77	0.85	0.32	-0.13	0.02
Br(3)	0.2083	0.2791	0.0203		1.14	0.82	0.63	-0.48	-0.01	-0.12
K	0.0115	-0.5283	0.2444	0.03	1.89	2.03	+1.06	-0.50	-0.19	-0.01

The temperature factors enter the structure factor calculation through the following expression:

$$\exp.\ (-10^{-2}(\beta_{11}h^2 + \beta_{22}k^2 + \beta_{33}l^2 + 2\beta_{12}hk + 2\beta_{13}hl + 2\beta_{23}kl)$$

TABLE C

The Observed and Calculated Structure Factors

	H	K	L	KLUE	F(ØBS)	F(CALC)	SIGMA
1	-7	-2	-9	0	35.79	41.76	4.30
2	-6	-3	-9	0	24.09	25.55	3.61
3	-5	-4	-9	0	41.14	42.20	5.15
4	-4	-5	-9	0	17.39	19.56	1.74
5	-3	-6	-9	0	35.73	41.08	4.87
6	-8	-0	-8	1	27.34	10.07	9.11
7	-7	-1	-8	0	30.31	20.48	10.10
8	-6	-2	-8	0	31.14	38.47	5.19
9	-5	-3	-8	0	48.67	52.50	4.73
10	-4	-4	-8	0	69.35	69.98	7.23
11	-3	-5	-8	0	68.83	71.13	7.17
12	-2	-6	-8	0	59.64	66.88	4.89
13	-1	-7	-8	0	30.31	54.45	10.10
14	-0	-8	-8	0	27.34	39.43	9.11
15	-8	1	-7	1	29.51	14.09	9.84
16	-7	-0	-7	1	31.24	21.57	10.42
17	-6	-1	-7	1	31.40	19.55	10.46
18	-5	-2	-7	0	31.28	27.57	10.42
19	-4	-3	-7	0	31.18	34.64	10.40
20	-3	-4	-7	0	31.18	34.83	10.40
21	-2	-5	-7	0	31.28	43.04	10.42
22	-1	-6	-7	0	31.40	33.57	10.46
23	-0	-7	-7	0	31.24	36.08	10.42
24	1	-8	-7	0	29.51	26.34	9.84
25	-9	3	-6	2	58.08	56.64	6.83
26	-8	2	-6	0	49.76	49.64	6.22
27	-7	1	-6	0	74.20	74.56	5.82
28	-6	0	-6	0	40.15	33.20	4.83
29	-5	-1	-6	0	49.14	47.71	5.05
30	-4	-2	-6	0	36.39	21.88	4.97
31	-3	-3	-6	1	28.74	1.47	9.57
32	-2	-4	-6	0	49.08	45.51	6.14
33	-1	-5	-6	1	30.47	8.74	10.16
34	-0	-6	-6	1	31.10	10.65	10.36
35	1	-7	-6	1	31.55	19.04	10.52
36	-8	3	-5	0	49.76	55.42	6.38
37	-7	2	-5	0	54.29	53.20	6.16
38	-6	1	-5	0	90.35	90.46	12.16
39	-5	-0	-5	0	76.02	71.56	7.59
40	-4	-1	-5	0	113.46	106.93	11.45
41	-3	-2	-5	0	70.46	67.29	7.05
42	-2	-3	-5	0	97.26	87.29	12.10
43	-1	-4	-5	0	44.13	42.53	4.91
44	-0	-5	-5	0	66.71	59.30	6.50
45	1	-6	-5	0	30.70	23.05	10.24
46	2	-7	-5	2	31.69	43.33	5.29
47	-7	3	-4	0	26.05	27.93	3.90
48	-6	2	-4	0	64.44	69.62	8.18
49	-5	1	-4	1	28.58	8.23	9.53
50	-4	-0	-4	0	177.40	183.59	29.83
51	-3	-1	-4	0	101.50	100.00	13.07
52	-2	-2	-4	0	213.30	280.23	35.14
53	-1	-3	-4	0	136.42	142.11	16.20
54	-0	-4	-4	0	207.53	219.44	34.78

KLUE: 0: means "observed"

1: means "unobserved"

2: means "unreliable"

	H	K	L	KLUE	F(ØBS)	C(CALC)	SIGMA
55	1	-5	-4	0	88.21	84.43	9.25
56	2	-6	-4	0	103.87	98.03	8.95
57	-3	7	4	1	31.91	22.13	10.64
58	-4	8	4	0	25.10	29.96	3.78
59	-6	3	-3	1	30.70	5.15	10.24
60	-5	2	-3	1	28.23	19.35	9.41
61	-4	1	-3	1	25.65	8.53	8.54
62	-3	-0	-3	0	56.04	46.65	5.59
63	-2	-1	-3	1	22.36	13.16	7.45
64	-1	-2	-3	0	93.61	96.49	7.11
65	-0	-3	-3	0	60.16	49.25	4.60
66	1	-4	-3	0	116.63	114.23	14.12
67	2	-5	-3	2	81.47	45.61	13.03
68	3	-6	-3	0	86.84	92.04	8.68
69	-4	7	3	1	32.19	23.87	10.72
70	-5	8	3	0	72.70	58.56	9.29
71	-7	5	-2	0	118.00	110.45	14.74
72	-6	4	-2	1	31.30	13.19	4.18
73	-5	3	-2	0	133.07	135.98	16.38
74	-4	2	-2	0	78.24	76.91	6.85
75	-3	1	-2	0	89.18	90.55	9.11
76	-2	-0	-2	2	129.21	251.06	15.93
77	1	-3	-2	0	48.00	36.24	4.73
78	2	-4	-2	0	100.94	99.33	7.43
79	3	-5	-2	0	82.86	84.62	6.58
80	-5	7	2	0	83.43	83.61	10.42
81	-4	6	2	1	31.30	6.65	10.44
82	-7	6	-1	0	77.51	61.47	9.90
83	-6	5	-1	0	58.55	48.55	7.61
84	-5	4	-1	0	108.83	99.70	10.72
85	-4	3	-1	0	99.30	102.05	7.33
86	-3	2	-1	0	125.49	128.72	15.63
87	-2	1	-1	0	118.93	142.89	19.55
88	1	-2	-1	0	27.59	26.25	3.45
89	2	-3	-1	2	54.83	54.11	4.46
90	4	-5	-1	0	60.63	46.25	7.69
91	3	-4	-1	1	26.11	11.47	8.70
92	-1	1	0	2	145.12	138.83	18.66
93	-2	2	0	2	215.65	379.90	25.53
94	-3	3	0	1	23.73	21.03	7.92
95	-4	4	0	0	149.77	150.45	19.61
96	-5	5	0	1	30.90	36.86	10.30
97	-6	6	0	0	59.35	53.56	7.71
98	0	0	2	0	135.46	144.69	17.03
99	0	0	4	2	210.22	399.43	26.30
100	0	0	6	0	59.15	48.93	7.67
101	0	0	8	0	169.48	181.21	21.12
102	1	1	0	0	143.56	138.83	17.90
103	1	1	2	1	64.86	17.84	8.10
104	1	1	4	0	106.42	104.69	16.07
105	1	1	6	1	30.59	11.98	5.89
106	1	1	8	0	82.73	78.37	10.21
107	1	1	10	1	36.28	12.32	6.98
108	1	1	12	0	50.62	52.55	6.07
109	-1	-1	4	0	117.23	133.08	17.64
110	-1	-1	8	0	104.44	105.05	12.95
111	-1	-1	12	0	69.81	68.49	9.11
112	2	2	0	2	217.89	379.90	27.44

	H	K	L	KLUE	F(ØBS)	F(CALC)	SIGMA
113	2	2	2	0	108.27	117.09	13.53
114	2	2	4	2	205.73	280.23	25.72
115	2	2	6	0	72.30	66.03	8.61
116	2	2	8	0	129.67	135.84	19.27
117	2	2	10	1	36.71	23.67	7.06
118	2	2	12	0	51.43	51.84	6.68
119	-2	-2	2	0	99.84	99.54	17.31
120	-2	-2	4	2	238.88	283.99	29.83
121	-2	-2	8	0	137.92	144.13	20.69
122	-2	-2	12	0	72.76	63.81	9.47
123	3	3	0	2	51.41	21.03	7.51
124	3	3	2	1	30.54	22.52	5.86
125	3	3	4	2	49.86	6.25	6.65
126	3	3	6	1	36.12	1.47	12.03
127	-3	-3	2	1	28.94	17.22	4.44
128	-3	-3	4	0	56.43	60.66	7.06
129	-3	-3	6	1	42.45	3.45	5.05
130	-3	-3	8	0	70.14	75.33	8.58
131	4	4	0	0	141.86	150.45	21.27
132	4	4	2	0	79.87	80.86	12.21
133	4	4	4	0	115.48	124.19	14.55
134	4	4	6	0	59.05	65.69	7.82
135	4	4	8	0	59.58	69.98	7.90
136	-4	-4	2	0	62.25	60.73	6.78
137	-4	-4	4	0	118.73	119.73	17.14
138	-4	-4	8	0	70.98	70.63	9.27
139	5	5	0	0	42.29	36.86	5.86
140	5	5	2	0	43.82	30.44	6.93
141	5	5	4	0	43.18	40.23	5.99
142	6	6	0	0	56.97	53.56	7.36
143	6	6	2	0	55.52	60.50	9.27
144	6	6	4	0	53.44	54.63	7.36
145	6	6	6	0	50.98	56.65	6.80
146	-6	-6	2	0	41.20	44.48	6.45
147	-2	-2	-5	0	51.41	36.50	8.81
148	-3	-3	-3	1	52.68	4.12	8.78
149	-3	-3	-7	0	54.48	24.96	18.48
150	-4	-4	-5	0	42.32	22.91	13.91
151	2	2	9	0	44.93	26.70	15.74
152	3	3	7	0	52.65	24.96	18.79
153	2	2	5	0	51.41	36.50	18.79
154	1	1	7	2	66.06	22.81	11.02
155	1	1	3	2	34.50	0.47	5.74
156	-2	-2	9	0	46.61	41.55	8.48
157	-2	-2	7	0	38.33	24.57	6.40
158	-3	-3	-7	1	47.29	0.16	7.90
159	-2	-2	5	0	49.20	51.10	8.43
160	-4	-4	5	0	50.67	49.52	8.45
161	-3	-3	3	2	47.19	12.66	7.87
162	-2	-2	1	0	26.83	21.71	4.75
163	-7	-1	-6	0	75.98	74.56	9.71
164	-6	-2	-6	0	58.22	54.80	7.83
165	-5	-3	-6	0	112.46	106.58	14.19
166	-4	-4	-6	0	73.01	65.69	9.56
167	-3	-5	-6	0	91.83	85.06	11.12
168	-8	1	-5	0	45.17	45.81	6.02
169	-7	0	-5	0	68.72	65.91	8.37
170	-6	-1	-5	0	96.14	90.46	11.86

	H	K	L	KLUE	F(ØBS)	F(CALC)	SIGMA
171	-5	-2	-5	0	116.30	110.68	14.29
172	-4	-3	-5	0	126.87	122.40	15.85
173	-3	-4	-5	0	117.73	121.60	14.71
174	-1	-6	-5	0	84.15	75.72	10.70
175	0	-7	-5	0	51.78	48.46	6.17
176	-2	-4	-4	0	52.53	45.26	6.34
177	-1	-5	-4	0	62.78	52.33	8.05
178	0	-6	-4	0	77.86	72.76	9.91
179	1	-7	-4	0	78.93	75.98	10.05
180	2	-8	-4	0	63.57	63.31	8.47
181	3	-9	-4	0	55.72	52.52	7.60
182	-3	-2	-3	0	33.19	25.21	4.43
183	0	-5	-3	0	63.42	56.39	7.75
184	1	-6	-3	0	41.85	38.41	4.93
185	2	-7	-3	0	71.62	71.27	9.16
186	-6	2	-2	0	72.81	68.03	9.61
187	-5	1	-2	0	57.90	43.57	7.06
188	-1	-3	-2	0	74.15	62.33	18.67
189	0	-4	-2	0	80.36	67.98	10.35
190	-7	4	-1	0	41.90	50.40	5.99
191	-6	3	-1	0	94.35	101.48	11.94
192	-5	2	-1	0	102.80	99.44	12.06
193	-2	-1	-1	2	51.44	142.89	6.56
194	0	-3	-1	0	61.52	61.73	7.60
195	-7	5	-0	0	73.92	79.05	9.01
196	-5	3	-0	0	112.04	115.66	13.99
197	2	-4	-0	0	43.04	50.54	5.75
198	3	-5	-0	0	112.41	142.88	13.97
199	-5	4	1	0	37.82	35.22	5.05
200	-4	3	1	0	35.61	32.75	4.95
201	-3	2	1	0	64.07	60.16	8.20
202	6	-7	1	0	72.09	58.45	9.21
203	-4	4	2	0	57.53	60.73	7.38
204	4	-4	2	0	87.37	80.86	22.31
205	5	-5	2	0	41.90	30.44	5.23
206	6	-6	2	0	61.10	60.50	7.63
207	-4	5	3	0	122.66	127.90	15.43
208	-3	4	3	0	50.64	42.89	6.34
209	-1	3	4	0	90.05	124.35	11.37
210	3	-1	4	0	105.25	100.00	30.96
211	5	-3	4	0	98.04	98.38	12.26
212	-1	4	5	0	104.93	112.95	13.22
213	0	3	5	0	81.65	74.63	19.86
214	4	-1	5	0	106.61	106.93	13.42
215	5	-2	5	0	95.79	110.68	11.84
216	6	-3	5	0	52.40	53.76	6.84
217	7	-4	5	0	53.34	49.78	6.34
218	2	2	6	0	77.27	66.03	9.66
219	3	1	6	0	78.11	71.42	9.76
220	5	-1	6	0	61.27	47.71	8.10
221	6	-2	6	0	57.45	54.80	7.45
222	-2	8	8	0	42.35	48.31	4.88
223	-1	7	8	0	59.98	57.08	8.07
224	0	6	8	0	65.58	62.49	8.20
225	1	5	8	0	59.34	49.41	7.70
226	2	4	8	0	58.77	48.74	7.63
227	0	7	9	0	47.23	43.36	5.89
228	1	6	9	0	66.84	64.51	8.35

	H	K	L	KLUE	F(ØBS)	F(CAL)	SIGMA
229	2	5	9	0	88.93	90.01	10.92
230	3	4	9	0	94.03	100.18	11.76
231	4	3	9	0	102.48	101.22	12.80
232	5	2	9	0	76.35	83.53	10.01
233	6	1	9	0	65.78	66.33	8.49
234	-3	-1	-2	0	94.38	90.55	11.94
235	-2	-2	-2	0	110.70	117.09	13.77
236	-4	0	-2	0	112.78	106.50	13.87
237	-4	1	-1	0	148.14	147.47	18.52
238	-3	0	-1	0	118.08	142.42	14.76
239	-1	-2	-1	2	91.90	134.89	11.59
240	1	-3	-0	0	117.01	155.73	14.71
241	1	-2	1	0	109.11	134.89	13.65
242	-2	2	2	0	108.84	99.54	13.60
243	-2	3	3	0	131.87	133.61	16.49
244	0	1	3	0	73.40	76.36	9.09
245	1	0	3	2	56.91	45.50	7.18
246	0	2	4	0	70.46	64.24	18.67
247	-3	1	-0	0	109.31	125.93	13.72
248	1	1	4	0	110.03	104.69	13.92
249	1	2	5	0	182.77	194.89	22.96
250	2	1	5	0	144.55	131.56	18.08
251	3	0	5	0	169.02	185.51	21.12
252	-8	-1	-5	0	46.26	45.81	6.61
253	-7	-2	-5	0	57.18	53.20	11.43
254	-6	-3	-5	0	64.41	53.76	6.51
255	-5	-4	-5	0	77.82	67.16	7.91
256	-4	-5	-5	0	56.31	47.51	6.08
257	-3	-6	-5	0	64.10	64.58	6.54
258	-2	-7	-5	0	39.98	34.11	5.45
259	-1	-8	-5	0	51.71	50.20	6.66
260	-7	-1	-4	0	53.10	34.52	13.70
261	-6	-2	-4	0	76.91	69.62	9.60
262	-5	-3	-4	0	95.79	98.38	11.55
263	-4	-4	-4	0	119.67	124.19	15.29
264	-3	-5	-4	0	122.37	126.02	15.24
265	-2	-6	-4	0	111.18	103.78	13.82
266	-1	-7	-4	0	87.71	83.48	9.07
267	0	-8	-4	0	43.26	44.00	5.84
268	1	-9	-4	0	42.44	32.23	5.55
269	-2	-5	-3	0	31.88	28.73	4.56
270	-1	-6	-3	0	35.96	36.36	4.49
271	0	-7	-3	0	44.08	40.83	5.52
272	1	-8	-3	0	45.41	39.38	6.05
273	2	-9	-3	0	43.05	35.35	5.38
274	-9	3	-2	0	60.68	72.66	12.78
275	-8	2	-2	0	47.15	51.85	9.98
276	-7	1	-2	0	91.02	88.58	9.41
277	-6	0	-2	1	27.73	13.59	10.39
278	-5	-1	-2	0	51.27	43.57	7.02
279	-4	-2	-2	2	79.10	76.91	10.15
280	-3	-3	-2	1	33.28	22.52	4.63
281	-2	-4	-2	2	106.76	100.43	10.66
282	-1	-5	-2	1	25.30	16.59	9.48
283	0	-6	-2	0	35.33	26.99	5.43
284	1	-7	-2	0	32.94	32.99	4.34
285	-7	2	-1	0	60.05	64.84	16.78
286	-6	1	-1	0	66.54	96.39	17.56

	H	K	L	KLUE	F(ØBS)	F(CALC)	SIGMA
287	-5	0	-1	0	80.36	109.14	20.69
288	-4	-1	-1	0	106.11	147.47	27.88
289	-3	-2	-1	0	135.80	128.72	22.62
290	-2	-3	-1	0	141.66	133.89	23.61
291	-1	-4	-1	0	95.31	83.69	11.94
292	0	-5	-1	0	75.56	73.75	9.62
293	-7	3	-0	0	30.36	26.28	3.79
294	-6	2	-0	0	96.51	91.72	12.03
295	-5	1	-0	1	66.30	21.30	8.49
296	-4	0	-0	0	184.39	247.20	30.75
297	1	-5	-0	2	60.92	69.15	9.79
298	2	-6	-0	0	116.80	118.10	14.59
299	3	-7	-0	1	30.36	0.01	11.38
300	4	-8	-0	0	41.34	38.76	5.16
301	1	-4	1	2	84.33	83.69	10.51
302	2	-5	1	2	72.71	76.49	9.19
303	3	-6	1	2	74.06	89.25	12.49
304	-7	5	2	0	78.86	91.18	9.98
305	-6	4	2	1	29.35	15.43	11.02
306	-5	3	2	0	95.98	105.92	9.62
307	-4	2	2	0	83.51	81.57	8.30
308	-3	1	2	0	48.23	63.01	6.03
309	2	-4	2	0	98.03	100.43	9.77
310	3	-5	2	0	89.35	112.35	9.00
311	5	-7	2	0	98.13	101.54	9.77
312	-7	6	3	0	73.99	64.74	9.26
313	-5	4	3	0	104.59	113.67	13.31
314	-4	3	3	0	62.73	64.34	7.86
315	-3	2	3	0	152.92	171.85	25.52
316	-4	4	4	0	112.43	119.73	13.99
317	-3	3	4	0	59.18	60.66	7.31
318	4	-4	4	0	122.20	124.19	15.46
319	5	-5	4	0	37.21	40.23	4.65
320	6	-6	4	0	55.97	54.63	7.64
321	-6	7	5	0	45.51	50.11	6.99
322	-5	6	5	1	33.04	9.98	12.40
323	-4	5	5	0	59.45	57.82	7.55
324	-3	4	5	0	32.87	26.53	8.20
325	-2	3	5	0	65.04	61.01	8.03
326	3	-2	5	0	73.55	67.29	9.21
327	4	-3	5	0	120.00	122.40	14.90
328	5	-4	5	0	67.57	67.16	9.14
329	6	-5	5	0	66.08	75.22	8.25
330	2	-1	5	0	133.03	131.56	44.33
331	0	1	5	0	117.59	90.49	39.26
332	-5	7	6	0	46.64	43.74	8.32
333	-4	6	6	1	32.85	16.07	12.32
334	-3	5	6	0	37.07	34.28	6.17
335	-2	4	6	0	49.08	46.66	8.83
336	3	-1	6	0	78.19	71.42	9.24
337	5	-3	6	0	101.82	106.58	13.51
338	7	-5	6	0	77.46	85.69	10.03
339	0	2	6	0	113.81	120.59	14.23
340	2	0	6	0	112.60	105.23	14.08
341	-3	6	7	0	59.50	69.11	6.95
342	-2	5	7	1	31.21	31.52	11.70
343	-1	4	7	0	92.44	93.98	11.70
344	0	3	7	0	47.68	37.86	6.10

	H	K	L	KLUE	F(ØBS)	F(CALC)	SIGMA
345	1	2	7	0	90.12	91.01	11.58
346	1	1	7	2	82.36	22.81	13.75
347	-3	7	8	0	38.59	35.95	6.10
348	-2	6	8	0	66.44	65.41	8.68
349	-1	5	8	0	77.37	73.13	9.43
350	0	4	8	0	123.93	120.04	15.92
351	1	3	8	0	92.87	93.52	11.33
352	2	2	8	0	137.27	135.84	17.12
353	3	1	8	0	65.62	61.34	8.03
354	4	0	8	0	82.53	89.08	10.47
355	6	-2	8	0	41.62	38.47	5.21
356	0	5	9	0	45.15	40.92	4.85
357	1	4	9	1	59.88	30.11	5.84
358	2	3	9	0	60.03	53.41	11.43
359	3	2	9	0	49.80	43.08	5.50
360	4	1	9	0	76.06	68.51	14.71
361	5	0	9	0	51.34	50.73	5.67
362	6	-1	9	0	63.43	66.33	6.03
363	-9	-3	-6	0	63.43	56.64	7.93
364	-8	-4	-6	0	42.23	39.29	5.86
365	-7	-5	-6	0	86.27	85.69	11.34
366	-6	-6	-6	0	65.50	56.65	8.20
367	-7	-5	-6	0	71.36	85.69	9.61
368	-8	-3	-5	0	52.45	55.42	7.00
369	-7	-4	-5	0	51.62	49.78	6.88
370	-6	-5	-5	0	85.58	75.22	11.20
371	-5	-6	-5	0	54.45	57.13	7.20
372	-4	-7	-5	0	62.53	73.93	7.81
373	-9	1	-2	0	45.96	40.69	6.20
374	-8	0	-2	0	37.55	31.62	4.68
375	-7	-1	-2	0	90.10	88.58	9.42
376	-6	-2	-2	0	73.65	68.03	9.10
377	-5	-3	-2	0	122.89	135.98	12.34
378	-4	-4	-2	0	87.46	80.86	8.83
379	-3	-5	-2	0	111.88	112.35	11.15
380	-2	-6	-2	0	44.26	40.16	4.66
381	-1	-7	-2	0	39.69	42.46	4.59
382	-9	2	-1	2	35.81	47.61	4.46
383	-8	1	-1	0	61.36	65.17	15.32
384	-7	0	-1	0	74.82	78.18	7.37
385	-6	-1	-1	0	97.32	96.39	9.81
386	-5	-2	-1	0	96.95	99.44	9.91
387	-4	-3	-1	0	123.35	102.05	26.37
388	-4	-3	-1	0	123.28	102.05	20.64
389	-3	-4	-1	0	109.66	95.26	18.27
390	-2	-5	-1	0	91.17	76.49	9.12
391	-1	-6	-1	0	70.68	63.69	7.37
392	0	-7	-1	0	34.81	44.12	7.90
393	-9	3	-0	0	44.23	41.82	4.61
394	-8	2	-0	0	41.64	36.56	4.00
395	-7	1	-0	0	43.62	43.37	4.85
396	-6	0	-0	0	42.57	35.26	4.64
397	0	-6	-0	0	79.68	75.77	7.90
398	1	-7	-0	2	99.29	91.14	15.98
399	2	-8	-0	0	58.92	64.55	6.81
400	3	-9	-0	0	66.36	62.70	7.37
401	-1	-5	0	2	109.15	69.15	18.30
402	1	-6	1	0	71.19	63.69	7.22

	H	K	L	KLUE	F(ØBS)	F(CALC)	SIGMA
403	2	-7	1	0	62.82	60.51	6.86
404	3	-8	1	0	35.30	41.25	3.93
405	0	-5	1	2	118.79	73.75	19.76
406	-8	4	2	0	42.33	40.10	5.29
407	-6	2	2	0	66.82	60.14	8.34
408	-5	1	2	0	31.59	34.66	3.51
409	-8	5	3	0	66.70	74.24	14.83
410	-7	4	3	0	45.67	43.25	5.71
411	-6	3	3	0	110.37	125.53	11.12
412	-5	2	3	0	61.36	58.82	6.15
413	-5	3	4	0	81.14	90.37	7.95
414	-4	2	4	0	57.09	58.77	5.86
415	3	-5	4	2	109.05	126.02	18.13
416	5	-7	4	0	70.21	83.31	9.56
417	-6	5	5	0	42.47	37.78	4.90
418	-5	4	5	0	42.86	43.27	5.05
419	-4	3	5	0	40.82	38.48	3.88
420	3	-4	5	2	105.52	121.60	17.69
421	4	-5	5	0	42.86	47.51	5.05
422	5	-6	5	0	55.23	57.13	5.66
423	-3	2	5	0	106.56	106.87	17.79
424	2	-3	5	2	143.74	87.29	23.88
425	4	-4	6	0	56.43	65.69	5.64
426	2	-2	6	0	90.49	66.03	14.74
427	-6	7	7	0	62.50	69.68	5.95
428	-5	6	7	0	38.01	34.87	4.22
429	-4	5	7	0	104.51	101.69	10.32
430	-2	3	7	0	81.53	85.62	8.03
431	-1	2	7	0	44.01	49.06	7.37
432	0	1	7	2	51.65	32.97	8.42
433	1	0	7	2	109.71	88.78	18.30
434	-4	6	8	0	57.09	53.73	5.71
435	-3	5	8	0	79.02	70.28	8.05
436	-2	4	8	0	84.09	84.32	17.37
437	-1	3	8	0	82.80	90.81	8.15
438	0	2	8	2	92.44	86.42	15.59
439	1	1	8	0	70.99	78.37	11.91
440	2	0	8	0	59.55	58.99	10.20
441	3	-1	8	0	69.87	61.34	6.68
442	4	-2	8	0	39.79	31.09	7.66
443	5	-3	8	0	50.48	52.50	5.61
444	-1	4	9	0	77.61	91.97	8.00
445	0	3	9	0	66.46	71.32	13.27
446	1	2	9	0	137.35	153.20	17.37
447	2	1	9	2	107.88	100.46	13.81
448	4	-1	9	0	78.78	68.51	10.51
449	5	-2	9	0	83.83	83.53	10.95
450	-1	7	12	0	55.19	40.31	14.74
451	0	6	12	0	66.55	45.32	8.32
452	1	5	12	0	42.28	42.84	5.88
453	2	4	12	0	39.62	40.78	4.95
454	2	5	13	0	64.53	56.33	8.08
455	3	4	13	0	64.55	60.98	16.15
456	4	3	13	0	70.70	60.59	8.83
457	5	2	13	0	43.28	49.16	6.00
458	6	1	13	0	43.18	39.47	6.00

Chapter 6

DESCRIPTION OF THE STRUCTURE

The final parameters of the refinement show that the $SnBr_6^{=}$ ion in K_2SnBr_6 has the configuration of a regular octahedron. There is no significant difference in the three non-equivalent Sn-Br distances and the angles between them do not vary significantly from 90° (Table D). The mean length of the Sn-Br bond is 2.601 ± 0.011 Å. Cruickshank[40] has pointed out that the measured bond lengths are usually shorter than the correct lengths. Since the atoms constituting the bonds are always in thermal motion, the positions of maxima in the electron density distribution do not represent the correct positions of atoms and so the measured bond lengths should be corrected for the thermal motion of atoms constituting the bonds.

In 1964, Busing and Levy[41] proposed a method for correcting the bond distances based on one of the following assumptions regarding the combined electron density distribution of two atoms forming the bond.

(i) the motions of atoms are either in phase or out of phase with one another.

(ii) The motion of the heavier atom is completely

TABLE D

Interatomic distances and angles

Atoms	Interatomic distance A Uncorrected	Corrected for thermal motion	Mean Corrected Value
$SnBr_6$ = ion			
1. Sn-Br(1)	2.579 ± 0.017	2.590	
2. -Br(2)	2.593 ± 0.008	2.603	2.601
3. -Br(3)	2.601 ± 0.008	2.611	
4. Br(1)-Br(2)	3.612 ± 0.020	3.612	
-Br(3)	3.754 ± 0.023	3.755	
-Br(2)	3.702 ± 0.018	3.704	
-Br(3)	3.569 ± 0.021	3.570	3.665
8. Br(2)-Br(3)	3.665 ± 0.012	3.666	
-Br(3)	3.679 ± 0.013	3.680	

Br(1)-Sn-Br(2)	88.58 ± 0.50
Br(1)-Sn-Br(2)	91.42 ± 0.60
Br(1)-Sn-Br(3)	92.90 ± 0.70
Br(1)-Sn-Br(3)	87.10 ± 0.59
Br(1)-Sn-Br(2)†	91.42 ± 0.60
Br(1)-Sn-Br(2)†	88.58 ± 0.50
Br(1)-Sn-Br(3)†	87.10 ± 0.59
Br(1)-Sn-Br(3)†	92.90 ± 0.70
Br(2)-Sn-Br(3)	89.78 ± 0.46
Br(2)-Sn-Br(3)	90.22 ± 0.42
Br(2)-Sn-Br(3)†	90.22 ± 0.42
Br(3)-Sn-Br(3)†	89.78 ± 0.46

The Br-Sn-Br angles lie within 2.9° of 90° and are not significantly different from it.

The errors quoted are those calculated from the standard errors for the cell constants and the least squares refinement.

† Those marked with a dagger are related by inversion through the origin.

independent of the motion of the lighter one, but the lighter atom is supposed to "ride" on the heavier atom.

(iii) There is no correlation between the motions of the atoms.

The first assumption gives the two extreme limits of the bond length, but the other two represent more physically likely situations. It is hard to distinguish between them unless detailed information about the motion of atoms is known. To convert isotropic to anisotropic motion of the atoms, the following relation is used

$$B_{ij} = 4\beta_{ij} / \underline{a_i^*} \cdot \underline{a_j^*}$$

cohere β's are the temperature coefficients, and B is the isotropic temperature factor.

The temperature factors (Table E) of the bromine atoms show a marked anisotropy indicating that their root mean square displacement perpendicular to the Sn-Br bonds is larger than that along the bonds. A rigid $SnBr_6^{=}$ ion liberating about the tin atom would give rise to anisotropy of this sort and if this were the case, the Sn-Br bond length corrected for temperature effects would be 2.60 Å. However, it is possible that there is no correlation between the motions of tin and bromine atoms. The thermal anisotropy of bromine atoms can be explained in this case, if we consider that the bending modes of vibration of the Sn-Br bond have larger amplitudes than the stretching modes. The mean corrected Sn-Br distance is then 2.63 Å. It is not possible

TABLE E

Principal Components of Temperature Factors

Atom	RMS(A)	Direction Cosines with respect to		
		a	b	c
Sn	0.125	0.000	0.000	0.000
	0.113	0.000	1.000	0.000
	0.106	0.000	0.000	0.000
BR(1)	0.223	0.894	0.448	0.015
	0.174	-0.382	0.780	-0.495
	0.106	0.233	-0.437	-0.869
BR(2)	0.222	-0.219	-0.043	0.975
	0.176	0.698	0.691	0.188
	0.112	-0.681	0.722	-0.122
BR(3)	0.207	-0.754	0.573	-0.322
	0.192	0.357	-0.054	-0.933
	0.112	0.551	0.818	0.164
K	0.265	0.597	-0.501	-0.627
	0.239	-0.284	0.599	-0.749
	0.200	0.751	0.625	0.215

to distinguish between these two cases and the true situation probably lies somewhere between the two extremes.

It is interesting to note that the positions of the $SnBr_6^{=}$ ions in the crystal are the same as those of $PtCl_6$ ions in the K_2PtCl_6 structure and $TeBr_6^{=}$ ions in the K_2TeBr_6 structure to which K_2SnBr_6 is closely related. The large octahedral ions lie on a face centered lattice with alkali metal ions occupying the tetrahedral cavities between them. In K_2PtCl_6 the $PtCl_6^{=}$ ions are all equivalent and are arranged with the Pt-Cl bonds along the principal axes of the cubic unit cell. The K_2SnBr_6 structure is obtained from this by a reorientation of the $SnBr_6^{=}$ octahedra as in the case of K_2TeBr_6.

The K_2PtCl_6 structure may be described as an approximately close packed array of chlorine and potassium atoms with platinum atoms occupying octahedral holes. The chlorine and potassium atoms are arranged with the array so that every potassium atom has twelve nearest neighbour chlorine atoms and every chlorine atom is surrounded by four potassium atoms, four chlorine atoms belonging to its own $PtCl_6^{=}$ ion and four chlorine atoms belonging to different $PtCl_6^{=}$ ions. In K_2TeBr_6, as reported by Brown, the environment of the halogen atom is only slightly altered but the environment of potassium atom is markedly different. The same is found to be the case for K_2SnBr_6 (Table F). It is possible to pick out twelve nearest neighbours for the pot-

TABLE F

Environment of K Atom

Atoms	Interatomic distance A Uncorrected	Corrected for Thermal Motion	Mean Corrected Value
K-Br(3)	3.132 ± 0.032	3.139	3.176
K-Br(2)	3.204 ± 0.031	3.213	
K-Br(1)	3.395 ± 0.050	3.404	3.462
K-Br(1)	3.510 ± 0.024	3.520	
K-Br(3)	3.736 ± 0.033	3.744	
K-Br(2)	3.868 ± 0.033	3.876	3.870
K-Br(2)	3.880 ± 0.033	3.886	
K-Br(1)	3.965 ± 0.024	3.974	
K-Br(3)	3.983 ± 0.033	3.992	
K-Br(2)	4.070 ± 0.032	4.078	4.077
K-Br(1)	4.083 ± 0.050	4.089	
K-Br(3)	4.141 ± 0.032	4.148	

TABLE G

Comparison of environment of K atom in K_2TeBr_6 and K_2SnBr_6

K_2TeBr_6				K_2SnBr_6			
	Interatomic distance A				Interatomic distance A		
Atoms	Uncorrected	Corrected	Mean Corrected Value	Atoms	Uncorrected	Corrected	Mean Corrected Value
K-Br(2)	3.37	3.40		K-Br(3)	3.132 ± 0.032	3.139	3.176
K-Br(3)	3.41	3.44	3.46	K-Br(2)	3.204 ± 0.031	3.213	
K-Br(1)	3.45	3.48		K-Br(1)	3.395 ± 0.050	3.404	3.462
K-Br(1)	3.48	3.51		K-Br(1)	3.510 ± 0.024	3.520	
K-Br(3)	3.61	3.64	3.84	K-Br(3)	3.736 ± 0.033	3.744	3.755
K-Br(2)	3.68	3.71	3.69	K-Br(2)	3.868 ± 0.033	3.876	3.870
K-Br(2)	3.65	3.68		K-Br(2)	3.880 ± 0.033	3.886	
K-Br(3)	3.71	3.74		K-Br(1)	3.965 ± 0.024	3.974	
K-Br(1)	4.10	4.13		K-Br(3)	3.983 ± 0.033	3.992	
K-Br(1)	4.16	4.19	4.16	K-Br(2)	4.070 ± 0.032	4.078	4.077
K-Br(3)	4.51	4.54		K-Br(1)	4.083 ± 0.050	4.089	
K-Br(2)	4.55	4.58		K-Br(3)	4.141 ± 0.032	4.148	

assium atoms but they are no longer equally distant. There are two bromine atoms at a distance of 3.176 ± 0.031 Å, then two at a distance of 3.462 ± 0.037 Å, four atoms at a distance of 3.870 ± 0.031 Å and the next four at a distance of 4.077 ± 0.037 Å. These bromine atoms are arranged such that the mean distance between any one bromine atom and the four potassium atoms with which it is associated is 3.755 ± 0.034 Å. The correction which should be applied to these lengths for thermal motion is about + 0.08 Å, if it is assumed that there is no correlation between the motions of potassium and bromine atoms. The comparison of the environment of the potassium ion in K_2TeBr_6 and K_2SnBr_6 is presented in Table G.

The distortion in K_2SnBr_6 is a result of packing large anions with small cations. The anions form a face centered array and are oriented such that each halogen is in contact with four halogens on neighbouring anions. This leaves cavities in the structure into which the cations fit. Each cavity is formed by twelve halogen atoms, three from each of the four anions which surround the cavity. The cations are usually much smaller than the halogen atoms Therefore, the size of the cavity will be determined by the halogen-halogen contacts between anions rather than the halogen-cation contacts. If the cation is very much smaller than the cavity into which it fits, it will be free to move inside the cavity unless the anions reorient them-

such as to reduce the effective size of the cavity and thus lock the cation into place.

The arrangement of cations (open circles) and anions (octahedra) in (i) K_2PtCl_6 (ii) K_2TeBr_6 and (iii) K_2SnBr_6 as viewed down the C-axis is drawn in Figure 6.

The stereographic projections of K atom are drawn in Figure 7.

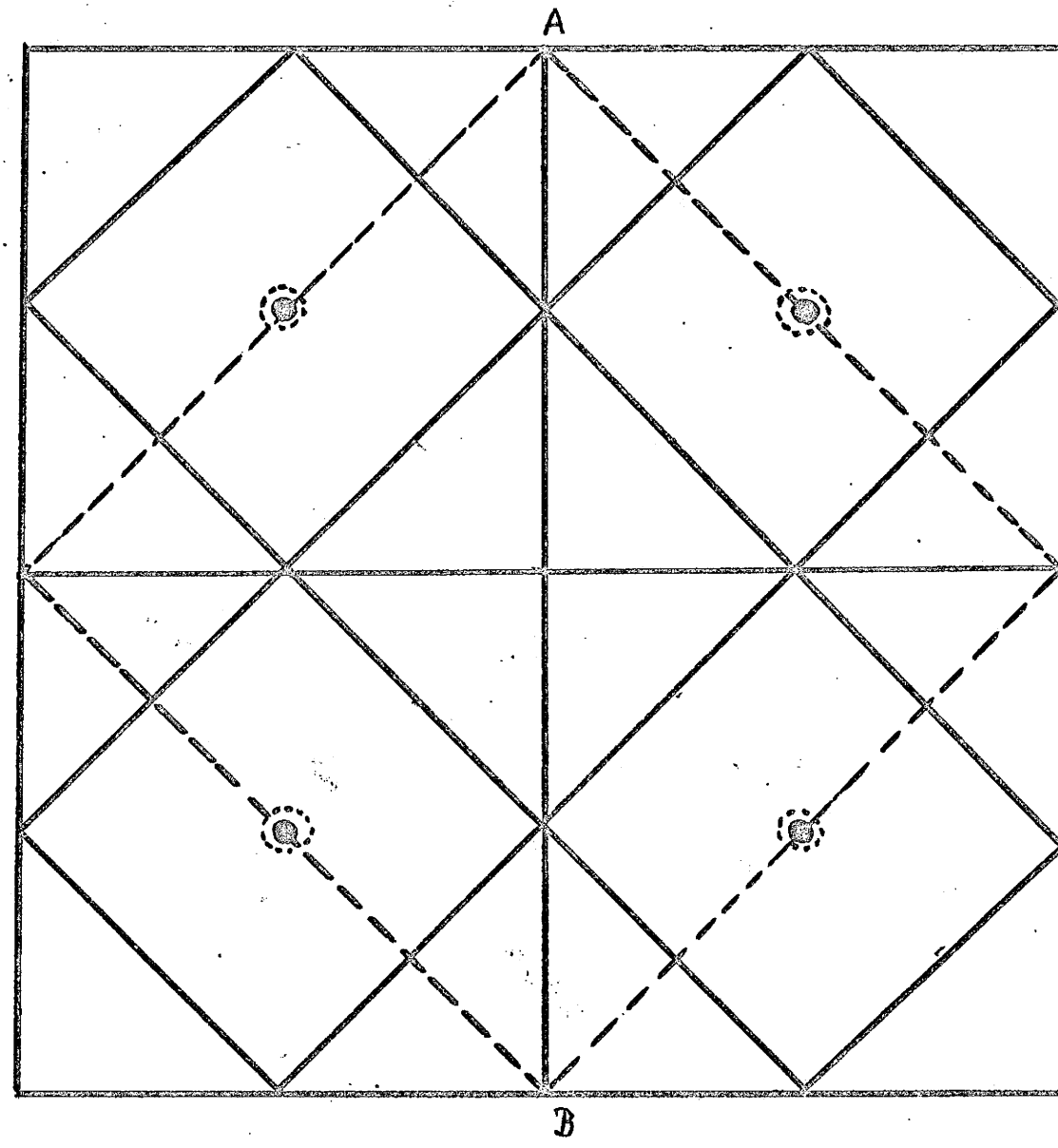

Fig. 6a. The arrangement of cations (open circles) and anions (octahedra) in K_2PtCl_6 as viewed down the C axis.

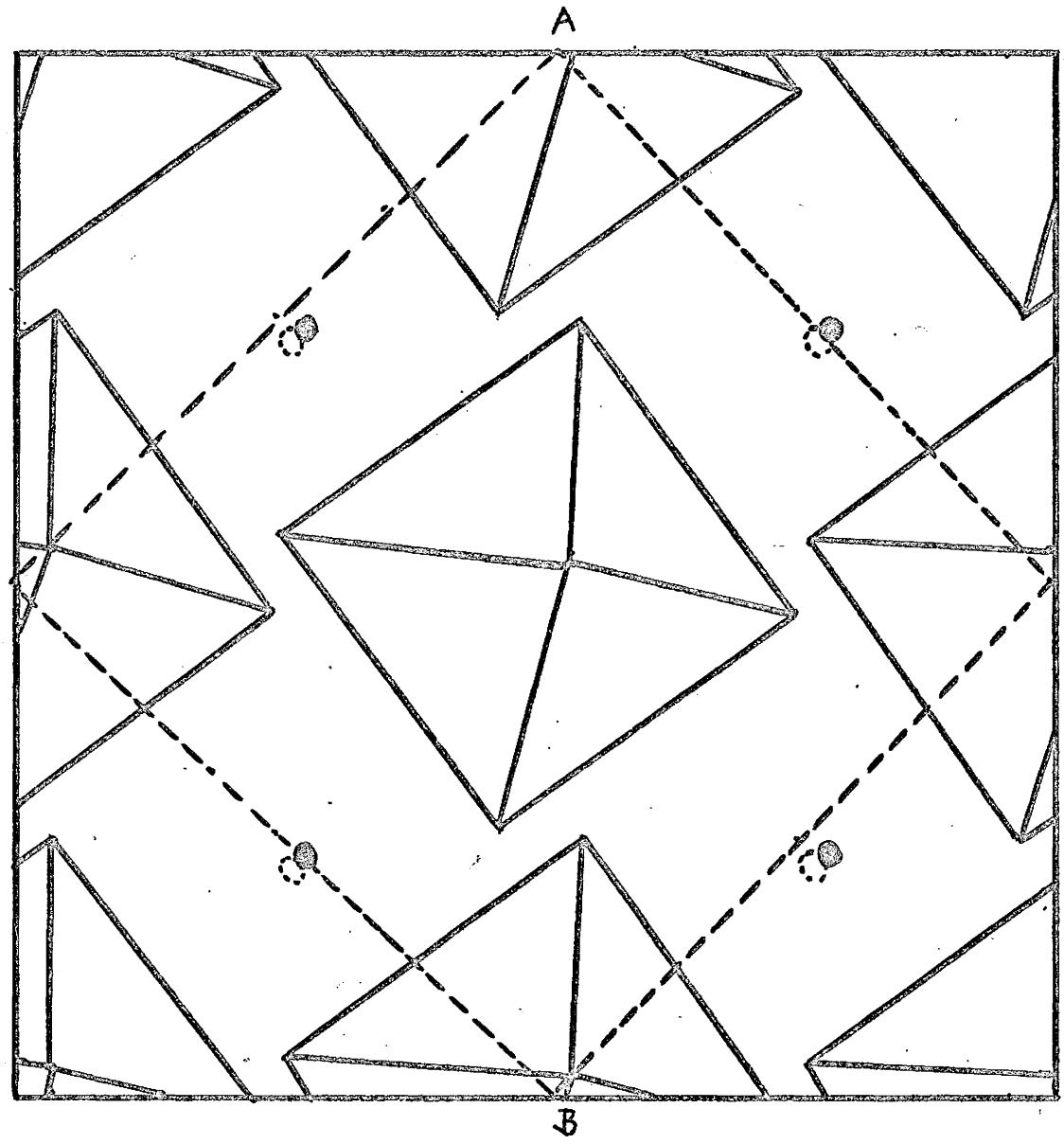

Fig. 6b. The arrangement of cations (open circles) and anions (octahedra) in K_2TeBr_6 as viewed down the C axis.

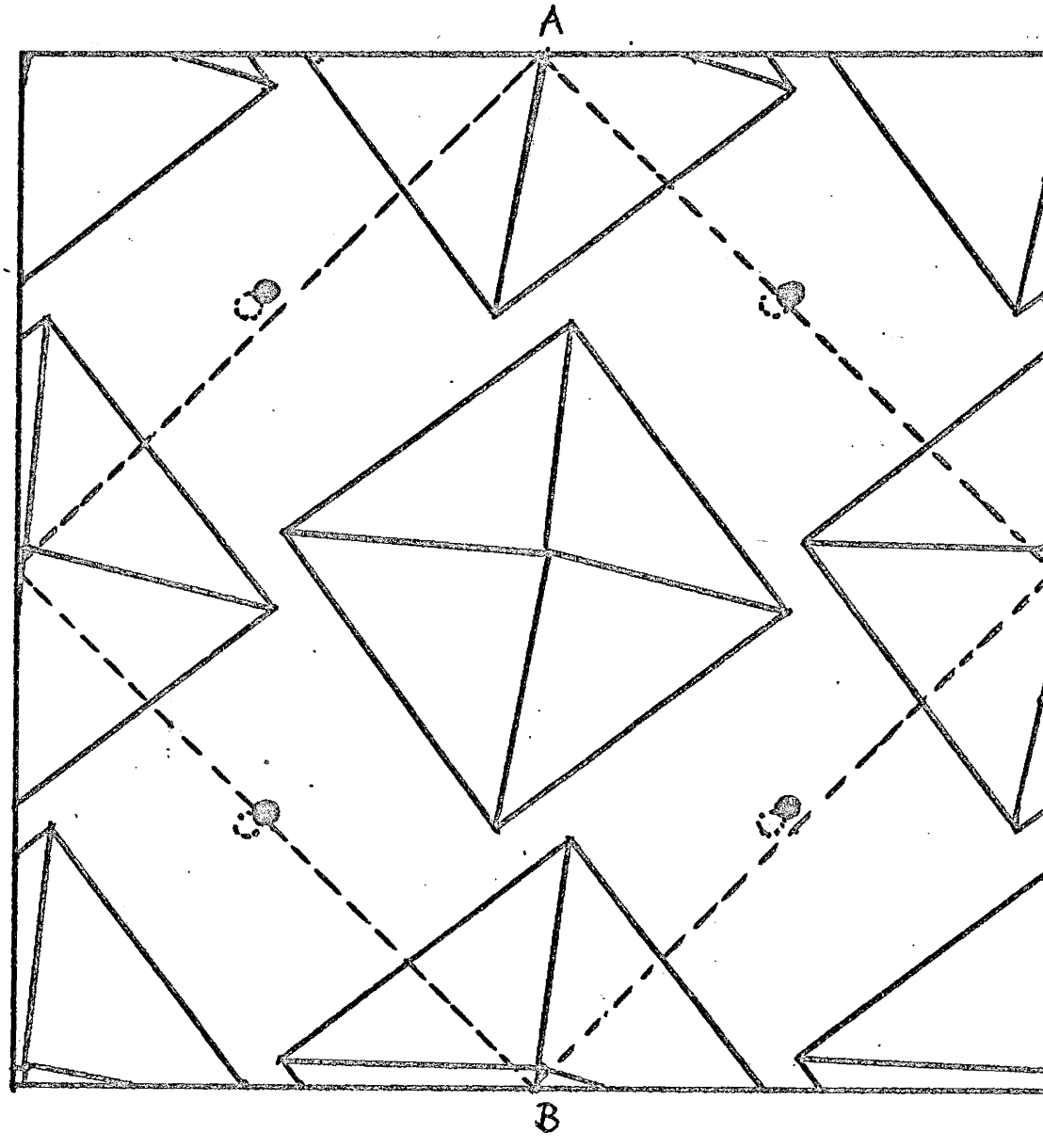

Fig. 6c. The arrangement of cations (open circles) and anions (octahedra) in K_2SnBr_6 as viewed down the c-axis.

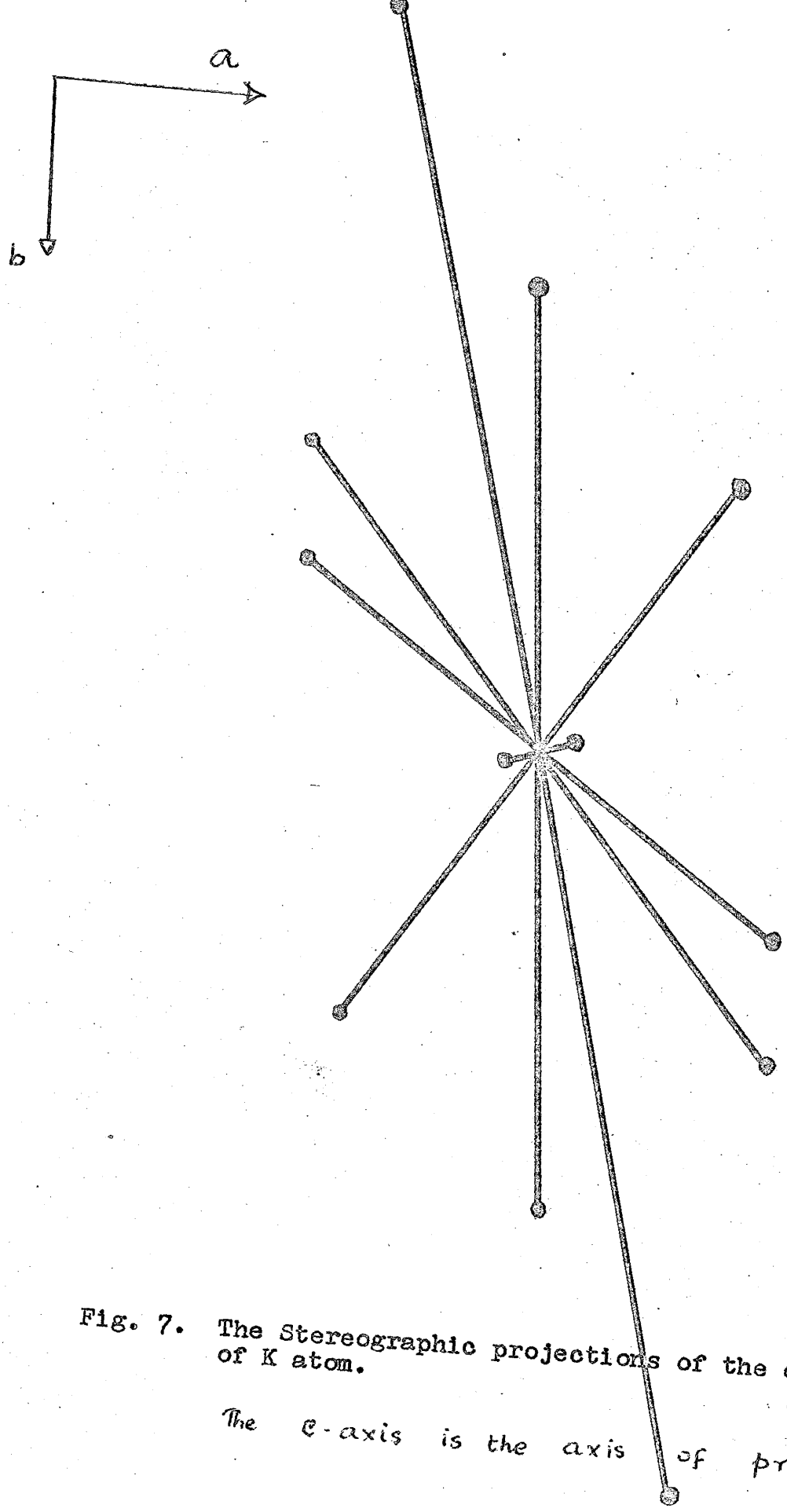

Fig. 7. The Stereographic projections of the environment of K atom.

The c-axis is the axis of projection.

BIBLIOGRAPHY

1. Ewing, F. J. and Pauling, L. (1928). Z. Krist, 68, 223.

2. Engel, G. (1935. Z. Krist. A 90, 341.

3. Hoard, J. L. and Dickinson, B. N. (1933). Z. Krist, 84, 436.

4. Sieg, L. (1932). Z. anorg. chem. 207, 93.

5. Bagnall, K. W., D'Eye, R. W. M. and Freeman, J. H. (1955). J. chem. Soc. 3963.

6. Templeton, D. H. and Dauben, C. H. (1951). J. Am. Chem. Soc. 73, 4492.

7. Brown, I. D. (1964). Can. J. Chem. 44, 2758.

8. Brown, I. D. and Lim, M. M. (1967). Can. J. Chem. 45, 678.

9. Ketallar, J. A. A., Rietdijk, A. A. and van Staveren, C. H. (1937). Rec. Trav. chim. 56, 907.

10. Markstein, G. and Nowotny, H. (1939). Z. Krist, 100, 265.

11. Galloni, E. E., De Benyacar, M. R. (1961). Anal. Acad. Nac. cien. c'ordoba (R.A.). 42, 241.

12. Nakamura, D., Kurita, Y., Ito, K. and Kubo, M. (1960). J. Am. Chem. Soc. 82, 5783.

13. Nakamura, D., Ito, K. and Kubo, M. (1962a). J. Am. Chem. Soc. 84, 163.

14. Nakamura, D., Ito, K. and Kubo, M. (1962b). Inorg. Chem. 1, 592.

15. Nakamura, D., Ito, K. and Kubo, M. (1963). Inorg. Chem. 2, 61.

16. Nakamura, D. and Kubo, M. (1964). J. Phys. Chem. 68, 2986.

17. Nakamura, D., Ito, K. and Kubo, M. (1961). Inorg. Chem. Vol. I, No. 3, 592.

18. Morfee, R. G. S., Staveley, L. A. K., Walters, S. T. and Wigley, D. L. (1960). J. Phys. Chem. Solids. 13, 152.

19. Busey, R. H., Dearman, H. H. and Bevan, Jr. R. B. (1962). J. Phys. Chem., 66, 82.

20. Smith, H. G. and Bacon, G. E. (1963). Acta. ryst. 16, A187.

21. Busey, R. H., Bevan, Jr., R. B. and Gilbert, R. A. (1965). J. Phys. Chem. 69, 3471.

22. Ikeda, R., Nakamura, D. and Kubo, M. (1963). Bull. chem. Soc. Japan, 36, 1056.

23. Ikeda, R., Nakamura, D. and Kubo, M. (1965). J. Phys. chem. 69, 2101.

24. Present work.

25. Galloni et al (1962). Z. Krist. 117, 407.

26. Werker (1939). Rec. Trav. chem. 58, 257.

27. Manjlovic' (1957). Bull. Inst. Nucl. Sci. "Boris Kidrich", Belgrade. 7, 79.

28. Das and Brown (1965). Can. J. chem. 44, 939.

29. Schwochau (1964). Z. Naturforsch. 19a, 1237.

30. Hazell (1966). Acta. chem. Scand. 20, 165.

31. Aminoff (1936). Z. Krist. 94, 246.

32. Manjlovic' (1956). Bull. Inst. Nucl. Sci. "Boris Kidrich", Belgrade. 6, 149.

33. Lipson, H. and Cochran, W. (1953). The determination of crystal structure, G. Bell and Sons, London, England, p. 11.

34. James, R. W. (1962). The optical principles of the Diffraction of x-rays. G. Bell and Sons, London England. p. 41.

35. Buerger, M. J. (1964). The precession method in x-ray crystallography. J. Wiley and Sons. Inc., New York, London, Sydney. p. 224.

36. International Tables for x-ray crystallography (1962). Vol. II. p. 302.

37. Buerger, M. J. (1960). Crystal structure analysis. J. Wiley and Sons Inc., New York. p. 103.

38. Nordman, C. E., Patterson, A. L., Weldon, A. S. and Supper, C. E. (1955). Rev. Sci. Instr. 26, 690.

39. Mellor, J. W. "A comprehensive Treatise on Inorganic and Theoretical Chemistry", Vol. 7 (1940), p. 456; B. Rayman and K. Preis: Ann. chem. 223, 326(1884).

40. Cruickshank, D. W. J. (1956). Acta. Cryst. 9, 757.

41. Busing, W. R. and Levy, H. A. (1964). Acta. Cryst. 17, 142.